Use Authorization

In presenting this thesis in partial fulfillment of the requirements for an advanced degree at Idaho State University, I agree that the Library shall make it freely available for inspection. I further state that permission to download and/or print my thesis for scholarly purposes may be granted by the Dean of the Graduate School, Dean of my academic division, or by the University Librarian. It is understood that any copying or publication of this thesis for financial gain shall not be allowed without my written permission.

Signature___________________________________

Date_______________________________________

FLOW MEASURMENT USING CRITICAL FLOW ORIFICES:

A Study of Their Limitations and Strengths

by

Joseph Berrett Maestas

A thesis

submitted in partial fulfillment

of the requirements for the degree of

Master of Science in the Department of Mechanical Engineering

Idaho State University

May 2016

Copyright

Committee Approval Page

To the Graduate Faculty:

The members of the committee appointed to examine the thesis of JOSEPH BERRETT MAESTAS find it satisfactory and recommend that it be accepted.

Dr. Richard Schultz,
Major Advisor

Dr. Ken Bosworth,
Committee Member

Dr. Bruce Savage,
Graduate Faculty Representative

Acknowledgement Page

I would like to show gratitude for all those who made this thesis possible. Thank you Idaho State University for the necessary resources required to produce this thesis. Thank you Dr. Brian Williams for brandishing those resources and helping me in the early stages. Thank you Dr. Ken Bosworth and Dr. Bruce Savage for providing comments and showing professionalism during my thesis defense. A very special thank you to Dr. Richard Schultz for mentoring me and providing expertise and support in the many hours dedicated to this thesis. And lastly, thank you Meranda Maestas for always believing in me, supporting me, and being my rock.

Table of Contents

List of Figures

List of Tables

List of Equations

Abstract

An experiment and analytical study were perfomed to determine the feasibility of building critical flow orifices for measuring mass flow rate using readily available machine tools (drill press and off-the-shelf drill bits), to determine whether an acceptable mass flow rate measurement could be achieved using standard analytical techniques, and to provide the uncertainties on the orifices, measurements, and instruments. Four sharp edge circular orifice plates with the following diameter hole sizes: 1/16-inch, 1/32-inch, 1/64-inch, and 1/64-inch with an exit chamfer were constructed and used as the basis for both the experiment and the calculations.

The work accomplished to both construct the critical flow orifices, assemble the experimental hardware and instrumentation, and conduct the experiments demonstrated that the effort required to use critical flow orifices is straightforward and relatively inexpensive. Certainly construction of critical flow orifices is considerably more straightforward than the design and construction of a critical flow venturi or nozzle—and the turnaround time and operational flexibility is overwhelmingly favorable to using critical flow orifices Therefore, on this basis, the overall evidence for using critical flow orifices is very favorable.

Measured mass flow rates were obtained using a collection tank downstream of the orifices.   Instrumentation such as differential pressure transducers and thermocouples along with a data acquisition system recorded both upstream and downstream conditions of the installed orifice plate. This data were used for both calculating and measuring the mass flow rate. Unfortunately the measured flow rates had unacceptably large uncertainties and therefore only provided qualitative data.

Based on the calculational uncertainties alone, which in general ranged from 1.5% to 2.9% for the Zucker equation, dependent on the size of the orifice, the results of this study show that critical flow orifices, which have the significant advantage of being simple to construct and install, offer a practical method for obtaining mass flow rates with a reasonably low uncertainty.

Chapter I: Introduction

There are many methods or devices used for the purpose of metering flow. These devices are designed and installed to measure the flow rate with measurement uncertainties explicitly defined in national standards. A common device known as an orifice meter, Figure 1, consists of a housing, orifice plate, and pressure taps. The orifice plate is inserted into the flow stream and creates a pressure drop across the orifice plate. The orifice meter measures this pressure drop in order to determine the mass flow rate of the stream. Orifice meters are relatively simple in construction and are less expensive than other flow meter devices, but they create large irrecoverable pressure losses. An orifice meter requires a pressure reading upstream and downstream of the orifice in order to obtain the flow rate, whereas a critical orifice meter only requires an upstream pressure reading.

Figure 1, Orifice Meter

Critical flow is a phenomenon that occurs when a pressure drop across the orifice is greater than the critical pressure ratio, which causes the mass flow rate to remain constant with a fixed upstream pressure, regardless of a varying downstream pressure.

Critical flow occurs when the speed of the fluid at the orifice is traveling at Mach 1. Mach 1 is a condition where the speed of the fluid is the same as the traveling speed of sound. This means that the sound waves travel at the same speed as the fluid. Sound waves are often referred to as pressure waves. A difference of pressure in a pipe or line causes a fluid to move through the pipe. If the fluid is moving at the same speed as the sound waves or pressure waves, then these pressure waves are unable to move upstream and cause the speed of the flow stream to increase. It can be said that the downstream is unable to communicate with the upstream. This phenomenon is known as choked flow or critical flow. This is why a critical flow orifice meter only requires an upstream pressure reading to determine the flow rate.

To assist in the understanding of building and operating critical flow orifices, an experimental apparatus was constructed and measurements of critical flow through four different orifice plates were obtained. The orifice plates were produced in a shop using readily available machinery and drill-bits. In summary, the objective of this project was to determine the feasibility of building critical flow orifices for measuring mass flow rate using readily available machine tools (drill press and off-the-shelf drill bits). This feasibility was determined by: (a) producing critical flow orifice plates, installing these orifice plates in an experimental apparatus designed to measure the mass flow rate and measuring the mass flow rate as well as (b) estimating both the measurement uncertainty for the critical flow experiments and the calculation uncertainty using standard uncertainty protocol approved by the American Society of Mechanical Engineers and available in their published standards

Operational Definitions

Critical Flow/Choked Flow, is a limiting condition where the mass flow rate will not increase with a further decrease in the downstream pressure environment while upstream pressure is fixed.

Critical Pressure Ratio, is the ratio of the downstream pressure to the upstream pressure of an orifice when critical flow occurs.

Data Acquisition System (DAQ), is a system that receives electrical signals from the thermocouples and differential pressure transducers and converts those signals into temperature and pressure readings.

Differential Pressure Transducer (DPT), is a device used for measuring the pressure difference between two locations in a system.

Discharge Coefficient, the ratio of the actual discharge to the ideal discharge. It is a coefficient used in an equation to account for discharge inefficiencies.

Orifice Plate, is a plate with an opening or hole that is placed in a flow stream to meter flow. Two types of orifice plates were used in the experiment and are described further in the *Description of Hardware* section.

Thermocouple, is a device used for measuring temperature.

Significance of the Study

The data and results obtained from this experiment will provide the necessary information to use a critical orifice plate as a flow metering device, and know the uncertainties associated with the flow meter. A critical orifice flow meter would be less expensive and a more simplistic option over other flow metering devices.

Chapter II: Literature Review

It is very important to review all available literature, studies, and experiments that are related to this topic. This will help determine if a similar project to this one has been investigated before, and what results and lessons were learned from that project. It may also provide valuable information and theory pertaining to this study. The scope of this literature review includes: (1) how critical flow orifices have been used historically, and (2) what are the key variables that relate to this study.

Critical orifices are more commonly used for the purpose of metering flow, but other purposes do exist. Busch provides a guide (Reference 1), on using orifices and nozzles for sizing vacuum pumps. The opening paragraph states, “Knowledge of the flow through an orifice and orifice size can be used in determining the sizing and selection of a vacuum pump or system. Many of the situations encountered when sizing vacuum equipment, particularly in material handling type applications are resolved with a basic understanding of how flow through an orifice works.” One application for this use of orifices with vacuum pumps, is the loading and unloading of boxes using suction cups, where each cup uses an orifice.

It is interesting to note that Busch reports a discharge coefficient of 61% for a sharp edge orifice, whereas the discharge coefficient of nozzle is reported to be 97%. This indicates that a sharp edge orifice is very inefficient. The guide provides a table for sizing a vacuum pump or system, but does not provide an equation to calculate flow for a specific scenario. There is also no information on the uncertainties associated with orifice plates or the measurements.

Another reference, C.H. Kurita, used critical flow restricting orifices in a building to limit the flow of nitrogen and air to the various users of the building. Kurita says, “These orifices are strategically positioned along the lines such that no one user can monopolize the gas supply and deprive others of air flow required to operate” (Reference 2). This reference reports a coefficient of discharge of 0.61, which correlates to the previous reference. However, the mass flow rate equation uses inlet conditions verses upstream conditions, and the equation seems to be simplified compared to other critical mass flow rate equations.

The results of Kurita’s experiment reported a difference of the calculated values compared to the observed values:

> While a part of this difference in the values can be attributed to experimental error, e.g. rotameter and pressure gage precision, the difference between the calculated and observed flow rates for plate “A” could be due to a geometry variance between the proposed design and final machined piece. The discharge coefficient for a shape edge orifice is 0.61 and that of a rounded edge orifice is 0.98. Upon close examination of the orifice plate, the edge appears to have more of a rounded than a sharp edge quality. Inserting the higher discharge coefficient value of 0.98 into the previously used sizing equation yields a flow rate value of 16.17 scfm, which is in better accordance with the empirically obtained value.

This reference makes the reader aware of measurement and instrumentation errors, but does not provide a guide for determining and calculating these uncertainties.

The next reference uses hypodermic needles as critical orifice meters for sampling ambient air. For this study, the hypodermic needle openings are approximately 20%

smaller than the tube diameter. It reports that the calculated critical flow rates have a maximum 5% error from the measured flow rates (Reference 3). Urone and Ross make this statement concerning critical flow:

> The ratio of the downstream pressure (P_2) to the upstream pressure (P_1) at which the critical flow rate as achieved is called the critical pressure ratio. Most studies report a critical pressure ratio of 0.5 is satisfactory for critical flow. Huygen, in studying the use of glass capillaries, showed critical orifice pressure ratios varying from 0.8 to 0.35 depending on the shape of the capillary. In this study it was found that a more conservative pressure ratio for hypodermic needles was 0.4.

This suggests that the critical pressure ratio can vary with geometry, and in order to be conservative, a lower pressure ratio should be assumed.

It was noted in a widely-cited paper by J. A. Perry: "Critical Flow Through Sharp-Edged Orifices" (see Reference 4) that:

> A very abrupt approach section, such as the square-edged orifice used in subsonic flow measurements, causes a choked flow condition that is affected by the pressure downstream of the device. Thus, at fixed inlet conditions, the mass flow can increase up to 11% as the downstream pressure is reduced from the value required to first establish sonic velocity, down to zero pressure. This is because of the changing shape of the contracting jet downstream of the orifice (vena contracta). Whereas this is a sonic flow device, it does not meet the essential requirement of a critical flow meter (i.e., that the mass flow is determined solely by the inlet conditions).

For this reason, this reference suggests that a square edge orifice does not meet the criterion of being a critical flow meter. However, all critical metering devices have errors and this specific error will be considered and be included in the total percent error calculation. Also, Perry's statement seems in opposition to more recently cited evidence given by A. J. Ward-Smith.

A. J. Ward-Smith (Reference 5), explores the critical discharge coefficient (Cd*). The The critical discharge coefficient is the ratio of the actual discharge over the theoretical discharge of an orifice. Equations have been derived from governing laws and then used to calculate the theoretical discharge of an orifice based on perfect conditions and no losses. The discharge coefficient is used to correct the calculated flow rate to match the actual flow rate. Ward-Smith presents a table of six combined references that list the critical discharge coefficient based on t/d, where t is the thickness of an orifice plate, and d is the diameter of the orifice. Ward-Smith also presents a graph of their own experimental results of a t/d range of 0.5 to 25, which shows that when t/d is between 1 and 7, the C_d value is constant. The 1/64-inch orifice plate (without an exit chamfer) that was used in this experiment, gives a t/d value of 8. This results in a slightly smaller C_d value as shown in Figure 2. For simplicity, it will be assumed that the C_d value for this orifice plate is the same as the others. Information from the Ward-Smith table relevant to this thesis research is summarized in

Table 1, and the graph from Ward-Smith is found in Figure 2. It should also be noted that the data given in Ward-Smith may be considered in agreement with that of Perry if orifices having a $t/d \leq 0.14$—since the data shown in Table 1 shows orifices with t/d ratios in this range did not choke. Further examination of these data may be fruitful.

Ward-Smith concludes the article by stating:

> The variations that exist (measurements fall in the band $0.81 < Cd^* < 0.86$) pinpoint two factors of crucial importance if this type of device is to be employed as a practical form of critical flowmeter. Firstly slight variation in the sharpness of the leading edge undoubtedly lead to variations in Cd*. Secondly, because the orifice diameters of interest are so small, even slight inaccuracies in the measurement of the internal diameter of the nozzle can lead to significant discrepancies in the estimation of mass flow rated. This second factor is of course shared by all designs of critical flowmeter, and not just those with sharp upstream edges. There is little doubt that, with care, the effects of both of these factors can be reduced to small proportions.

Table 1, Critical Discharge Coefficients

References	t/d	Cd
Brain and Reid (Ref 6)	0.28	0.841
	0.31	0.83
	0.488	0.844
	0.50	0.83
	0.51	0.83
	0.51	0.839
	0.54	0.845
	0.92	0.825
	0.986	0.835
	1.01	0.83
	1.01	0.83
	1.02	0.845
	1.933	0.82
	1.97	0.825
	2.00	0.841
	2.00	0.832
	2.07	0.843
	3.48	0.839
	4.92	0.826
Deckker and Chang (Ref 7)	2	0.86
	1	0.86
	0.5	0.88
Jackson (Ref 8)	0.33	0.845
	0.67	0.86
	1.0	0.835
	5.3	0.84
Grace and Lapple (Ref 9)	1.00	0.83
Kastner, Williams, and Sowden (Ref 10)	1.45	0.83
	1.473	0.832
	1.476	0.84
	1.433	0.832
	1.543	0.829
Rohde, Richards, and Metger (Ref 11)	4.00	0.85
	2.83	0.86
	2.00	0.86

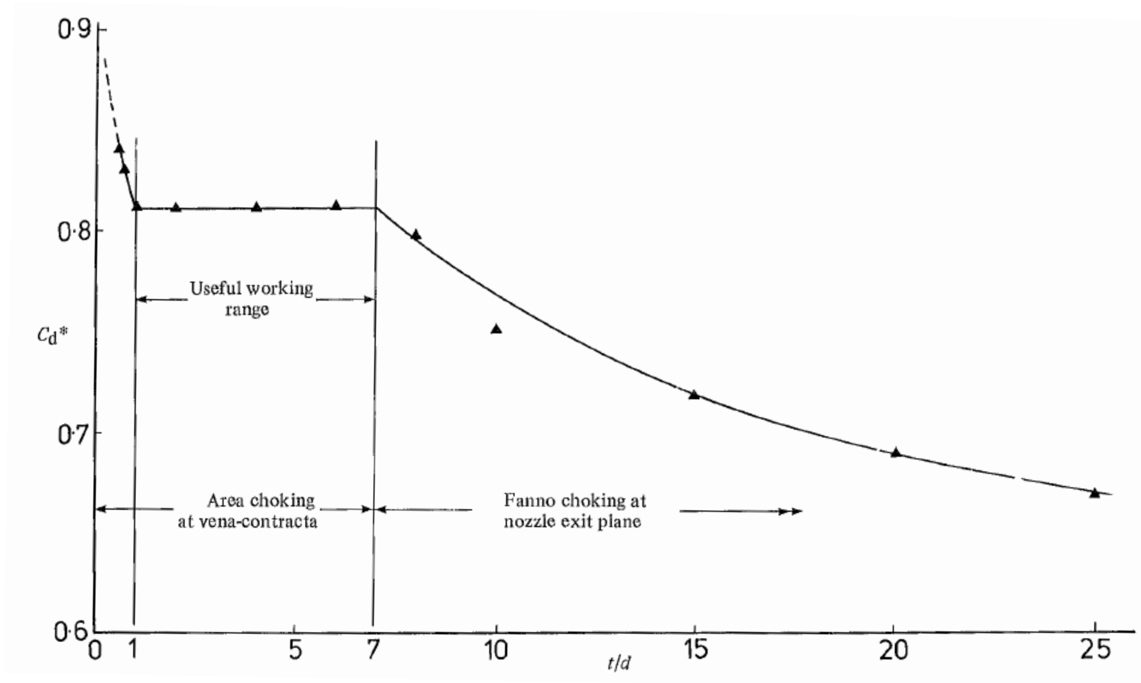

Figure 2, Graph showing the relationship between Cd and t/d (Fig 7 in Ward-Smith, Ref 5)

Ward-Smith states that variations in the discharge coefficient will exist due to the sharpness of the leading edge of the orifice and from inaccuracies in measuring the internal diameter of the orifice.

It was mentioned that critical orifice meters produce irrevocable losses. One source of loss or inefficiency in this flow meter is in the form of a shock wave. A shock wave forms when the speed of the fluid changes by more than the speed of sound. The sound waves travel upstream against the flow and reach a point where they cannot travel any further. This causes the pressure in this region to increase until a pressure shock wave forms. A shock wave takes the form of a very sharp change in the gas properties: density, temperature, pressure, velocity, and Mach number. For this reason, the presence of a shock wave also makes it very difficult to obtain accurate pressure and temperature readings. For this reason, no pressure or temperature readings will be taken close to exiting flow of the orifice plate.

Perry (Reference 4) also comments on shock waves, “Losses are caused by fluid friction losses from turbulence (vortices) and losses across shock waves in addition to boundary layer losses... A related disadvantage of the critical flow meter is the acoustical disturbance created in the downstream fluid. At the high end of the flow range, with low downstream pressure, the exit velocities can be in the high supersonic range. The resulting shock waves cause acoustical noise and turbulence, which may affect apparatus performance and downstream measurements in some applications. Special attention must be paid to this potential problem in calibration activities.” Perry states that losses accompany choked flow in the form of shock waves, and that these shock waves will affect instrumentation readings. The downstream pressure and temperature was measured away from the orifice exit, so as to decrease or eliminate instrumentation noise. If an efficient metering device is desired where losses need to be minimal, a critical orifice meter should not be used.

The next reference, Zimmerman and Reist (Reference 12), state that there are three major limitations to the critical orifice meter. These limitations must be understood in order to provide a successful and accurate way of metering flow:

> First, particulate matter in the airstream may partially block the throat opening and totally alter the flow characteristics. Second, the critical orifice must be calibrated for each specific sampling situation since the flow rate is directly proportional to the upstream absolute pressure and sampling device upstream may change the calibration. Finally, and most importantly, the vacuum supply (pump)

must have sufficient capacity to ensure that the throat velocity remains sonic and hence the flow remains constant.

The first limitation will not be an issue for this experiment, because nitrogen gas from a bottle will be used and no particulate matter will be present in the system. The second limitation is basically the scope of this paper. The experiment will give insights regarding the accuracy of the flow measured using each orifice plate. The third limitation will be monitored by differential pressure transducers, to ensure that the flow remains critical or choked.

The article also has information regarding the critical pressure ratio, "In 1886 Reynolds' theoretical and experimental studies indicated that for the characteristics of ambient air, the flow through a sharp-edge orifice would remain constant if $R_{cr} \leq 0.527$." This critical pressure ratio value only applies to ambient air through a sharp-edge orifice. The value will be different for other fluids and orifice types. nitrogen's critical pressure ratio, as reported from other sources, is 0.528 for a sharp edge orifice. This source suggests that the critical pressure occurs at a given value and not within a range. However, this reference does not mention if that value would change if the orifice were slightly rounded versus sharp edged. To guarantee that the experiment maintains choked flow, the pressure ratio will not be close to or approach the 0.528 value.

Zimmerman and Reist also state that the critical pressure ratio is affected by the orifice type. The article cites T.E. Stanton, see Reference 13:

> Stanton continued the comparison of orifice shapes and found that R_{cr} appeared to vary depending on orifice configuration, pressure measurement location and extent of vena contracta formation. He concluded that the sonic air jet did not fill

the entire throat area, with the exception that the minimum jet section could be regarded as identical to the throat of a venture-shaped converging-diverging orifice.

The article includes a table of R_{cr} values for different orifice configurations. These values range from 0.44 to 0.87. As previously mentioned, this experiment will assume that the critical pressure ratio is 0.528, but will avoid approaching close to this value so as to maintain choked flow.

Summary

The literature review mentions five important topics that can be summarized below:

1. Orifice meters produce inefficiencies and losses, and shock waves effect instrumentation.
2. In order to have an accurate orifice meter, the orifice must be calibrated for its setting and application.
3. The critical pressure ratio must be obtained with a Mach number of 1 at the minimum area of the vena contracta downstream of the orifice, in order to produce critical flow and a constant mass flow rate, but “the mass flow can increase up to 11% as the downstream pressure is reduced from the value required to first establish sonic velocity” (Reference 4).
4. A discharge coefficient takes into effect a non-ideal flow and is used in a theoretical equation to predict the actual flow.

5. The accuracy of the results is very dependent on the sharpness of the leading edge of the orifice, and using the actual size of the orifice in the calculation process.

Chapter III: Description of Hardware

This section includes information about the hardware, its manufacturer, model number, range, and the measurement uncertainties if applicable. This information can be used to replicate this experiment or obtain further information on the hardware. A hardware identification photograph and table, as shown in Figure 3, shows where the hardware is located and lists the hardware's manufacturer, model number, and range. A piping and instrumentation diagram, as shown in Table 2, shows how the hardware and instruments connect together. A table summarizing all of the lines lengths and inside diameters can be found in Appendix E.

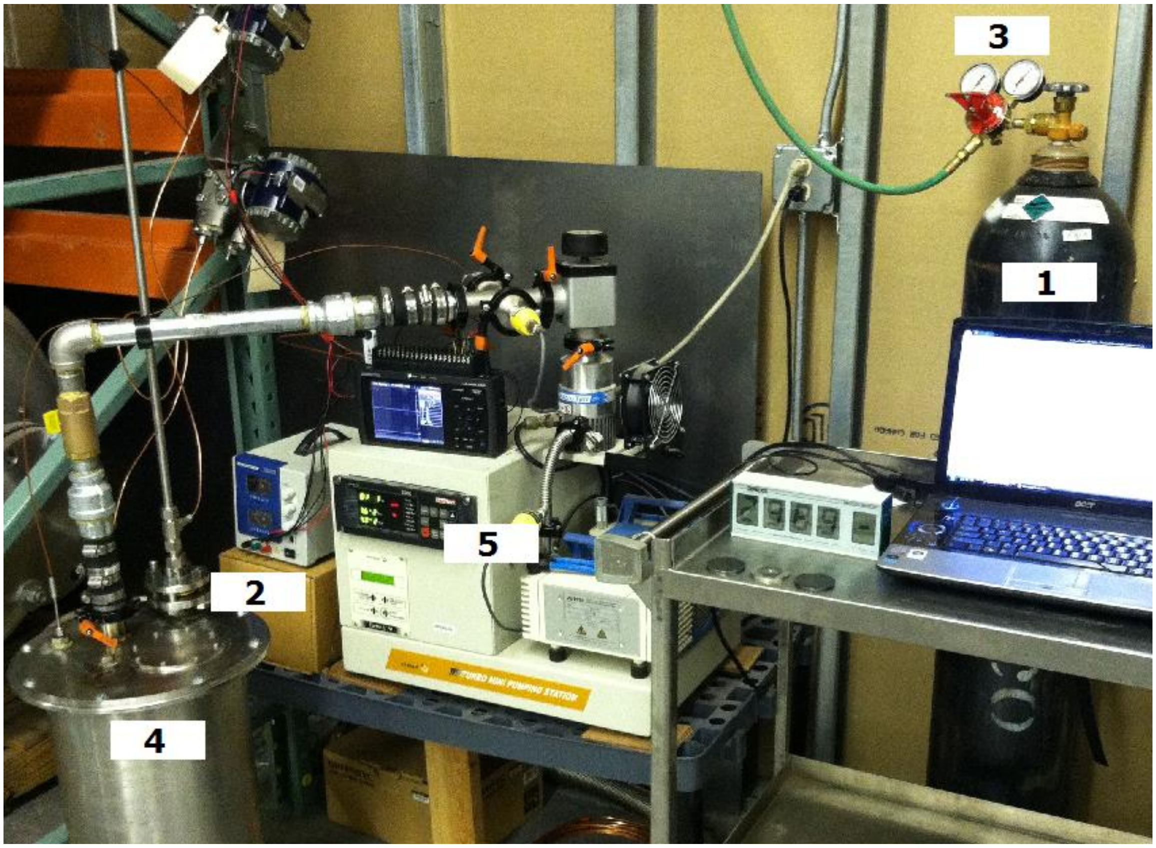

	Name	Manufacturer	Model Number	Range
1	Nitrogen Tank	Norco	NA	NA
2	Orifice Plate	NA	NA	NA
3	Pressure Regulator	Smith	30-100-540	0-3000 psi
4	Receiver Tank	NA	NA	NA
5	Vacuum Pump	Varian	Turbo-V-70	1x10^-9 Torr

Figure 3, Hardware Identification

Table 2, Piping, Hardware, and Instrumentation Diagram

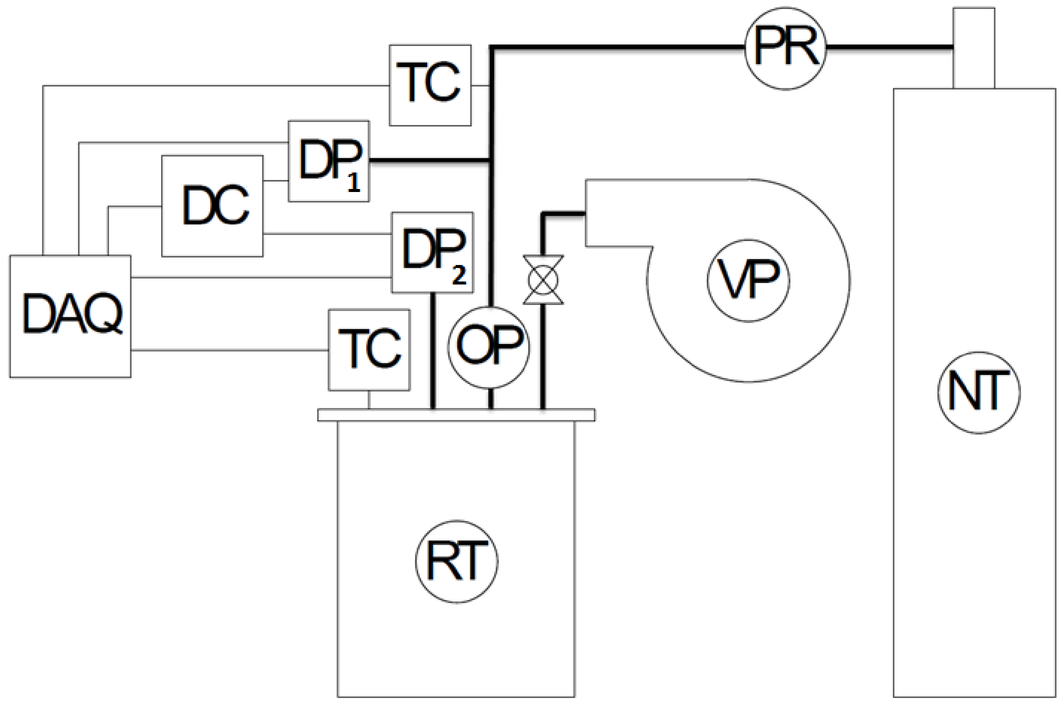

□	Instrument
○	Hardware
⌧	Valve
—	Nitrogen Line
–	Instrument Electrical
DAQ	Data Acquistion System
DP_1	Differential Pressure Transducer (25 psid)
DP_2	Differential Pressure Transducer (300 inch)
TC	Thermocouple
DC	DC Power Supply
NT	Nitrogen Tank
OP	Orifice Plate
PR	Pressure Regulator
RT	Receiver Tank
VP	Vacuum Pump

A gas bottle is to provide pressured nitrogen as the working fluid for the experiment. Air is 78 percent nitrogen, which is a close approximation for pure nitrogen, but to render more accurate results, 99.99% pure commercial grade nitrogen gas will be used as the test gas. A nitrogen bottle, provided by the company Norco, was used as the source of nitrogen for this experiment. The pressure just upstream of the orifice was maintained at around 20 psig using a regulator.

An orifice plate, as shown in Figure 4, was constructed with a hole drilled in the center of a circular plate with the desired drill bit size.

Figure 4, 1/64-inch Diameter Orifice Plate

L.K. Spink, Reference 14, lists specifications for the sharp, square-edged, thin-plate concentric orifice which is shown in Figure 5. Specification number one was ignored for the 1/16-inch, 1/32-inch, and the 1/64-inch diameter orifice plates. This was done to simplify the fabrication process and to make it easier to duplicate the results. Table 3 shows the how the orifice plates deviate from Spink's requirement. Furthermore, the data of Ward-Smith indicates that specification number one is not essential. All of the other specifications were followed.

Table 3, Spink's specification number one

	Plate Specification (inches)			
	Thickness	d/8	D/50	(D-d)/8
1/16-inch	0.125	0.00781	0.0086	0.0459
1/32-inch	0.125	0.00391	0.0086	0.0498
1/64-inch	0.125	0.00195	0.0086	0.0518

THE SHARP, SQUARE–EDGED, THIN–PLATE CONCENTRIC ORIFICE

In order to use the published coefficient data within the standard tolerances, the orifice should be made to the following specifications in which d = orifice diameter and D = pipe diameter:

1. The thickness should not exceed any of the following limits: $d/8$, $D/50$, or $(D-d)/8$, in the cylindrical portion. If a thicker plate is required for rigidity, the outlet face may be beveled or recessed to attain the desired dimension. This should be done in such a way that a straightedge laid across the bevel or recess will form an angle not less than 45° to the axis of the pipe.
2. The upstream edge should be square and as sharp as possible. Any rounding should not exceed 0.025% of the diameter of the orifice to assure measurement within 0.1%.
3. The upstream face should be at least as smooth as good commercial rolled stock.
4. The portion of the plate which extends inside the pipe should be flat within 0.01″ per inch of radius.
5. The orifice plate should be centered in the pipe in such a way that the eccentricity is less than 3% of the pipe diameter.

Figure 5, Orifice Plate Specifications

Four orifice plates were constructed: 1/16-inch hole, 1/32-inch hole, 1/64-inch hole, and a 1/64-inch hole with an exit chamfer. The 1/64-inch hole with the exit chamfer has a 45 degree chamfer to the axis of the pipe. The plates are approximately 2 inches in diameter and are made out of 1/8-inch thick cold rolled, low carbon steel. The d/D values are as follows: 1/16-inch -> 0.1453, 1/32-inch -> 0.07267, and 1/64-inch -> 0.0372, where D is the inside diameter of the entrance line, and d is the diameter of the drill bits. The t/d values are as follows: 1/16-inch -> 2, 1/32-inch -> 4, 1/64-inch ->8, and 1/64-inch Chamfered -> 2 where t is the thickness of the of the plate at the orifice, and d is the diameter of the drill bits. The drill bits were purchased at Tacoma Screw Products, and the orifice plates were cut out on a CNC plasma table, and the holes were drilled with a drill press.

The method used to verify the orifice area and level of uncertainty on the area is known as pixel counting. This procedure is discussed in the Appendix A. The level of uncertainty of the orifice area and diameter is shown in Table 4.

Table 4, Uncertainty of Orifice Area and Diameter

Uncertainty of Orifice Area				
1/16 inch	0.00307	+/-	0.000167	in^2
1/32 inch	0.000767	+/-	0.0000833	in^2
1/64 inch	0.000201	+/-	0.0000416	in^2
Uncertainty of Orifice Diameter				
1/16 inch	upper limit		0.06420	in
	lower limit		0.06080	in
1/32 inch	upper limit		0.03290	in
	lower limit		0.02950	in
1/64 inch	upper limit		0.01758	in
	lower limit		0.01425	in

A pressure regulator was required for the experiment to provide a constant upstream pressure. The orifice mass flow rate will only remain constant if the upstream pressure remains constant. A pressure regulator was fitted on the nitrogen bottle and was set to 20 psig. The pressure regulator used is a Smith model number 30-100-540 with a 3000 psig max pressure inlet, a 0-100 psig delivery pressure, and a +/- 2% of actual gauge reading for both the pressure regulator and flow gauges.

A receiver tank was also required to collect and contain the nitrogen passed from the orifice plate. This receiver tank was constructed to withstand a negative pressure, close to a perfect vacuum, with only a negligible change in volume. The tank was fabricated for another experiment, but modified for this experiment to house all of the required fittings. It was constructed of ¼-inch thick stainless steel with a groove for an O-ring to seal the lid to the body. The volume of the receiver tank, and the remaining volume downstream of the orifice plate was found to be 0.94758 ft^3, and the uncertainty was found to be +/- 0.00247 ft^3. The procedure for measuring the volume and determining its uncertainty can be found in Appendix A.

A vacuum pump was used for this experiment. It was connected to the receiver tank with a valve in between the receiver tank and the vacuum pump. The valve was closed during testing, which limited the control volume to that downstream of the valve. A Varian Turbo-V-70 vacuum pump was used with k-type vacuum fittings. These fittings use a tightening collar and a rubber O-ring gasket. The rubber O-ring gasket should have vacuum grease applied to it, to seal and help prevent leaks. The vacuum pump must be able to remove the majority of air from the receiver tank to produce accurate results. The vacuum manufacturer reports being able to reach vacuum pressures as low as 1×10^{-9} Torr, however these pressures were never reached. While purging the experimental apparatus of air, the pressure would reach 3×10^{-3} Torr which is equivalent to 5.8×10^{-5} psi. It was calculated, using the ideal gas equation, that the amount of air that remained after evacuating the experimental apparatus after one purge was 2.70751×10^{-7} lbm. A second purge was performed to reduce that amount to practically zero.

Chapter IV: Description of Instrumentation

This section includes information about the instrumentation used with the instrument's manufacturer, model number, range, and its measurement uncertainty. This information can be used to replicate this experiment or obtain further information on the instrumentation. Below is an instrumentation identification photograph and table, as shown Figure 6, that shows where the instruments are located and the instrument's manufacturer, model number, range, and uncertainty. A piping and instrumentation diagram, as shown in Table 2, shows how the hardware and instruments connect together.

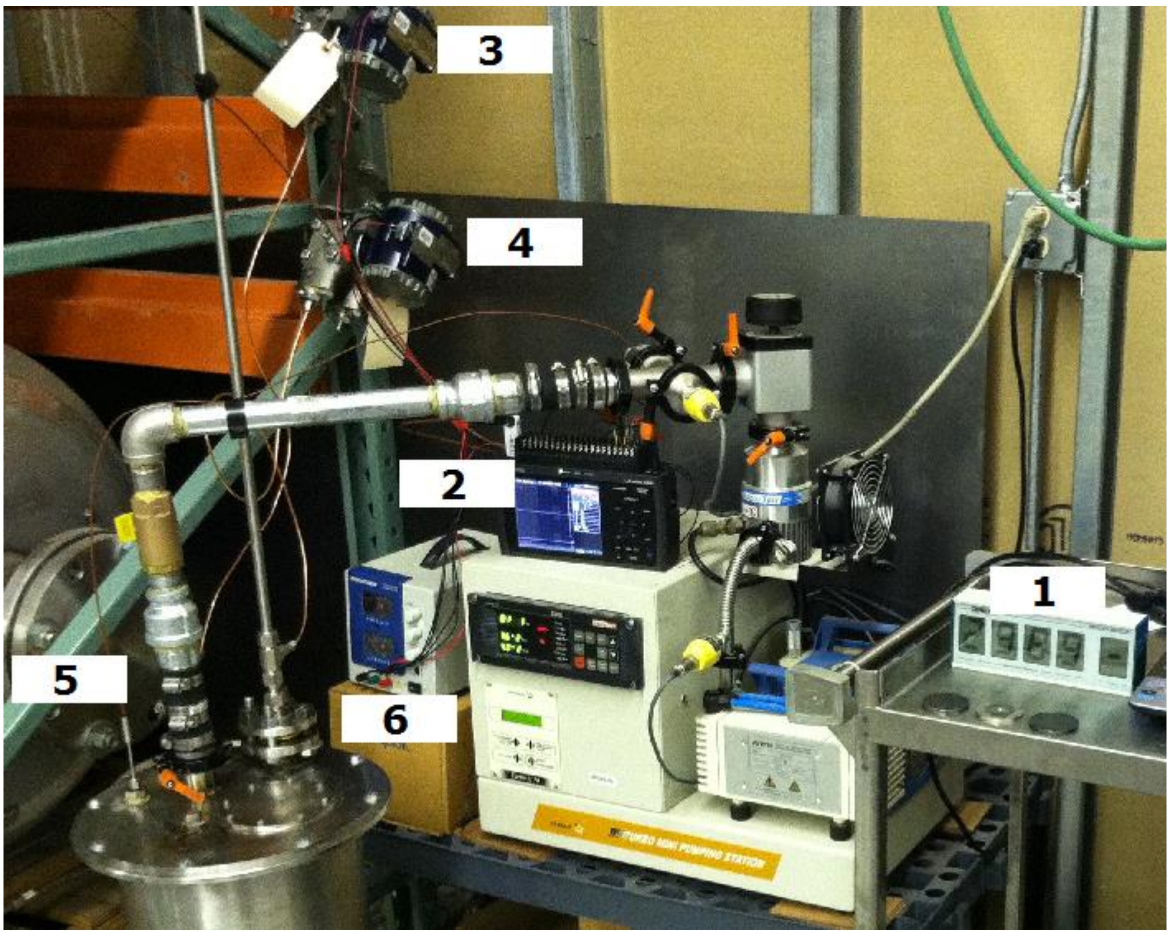

	Name	Manufacturer	Model Number	Range	Uncertainty	
1	Barometer	Conex Electro-Systems	Model JDB-1	9.8-15.2 psia	+/-	0.025 psi
2	Data Acquistion System	Graphtec Corp.	Midi Logger GL820	0-50 volts	+/-	0.05 volts
3	300 inch H20 Differential Pressure Transducer	Omega Engineering	PX771A-025DI	0-10.84 psi	+/-	0.01626 psi
4	25 psid Differential Pressure Transducer	Omega Engineering	PX771A-300WCDI	0-25 psi	+/-	0.0375 psi
5	K Type Thermocouples	Idaho Laboratories Corp.	K-Type	0-150°F	+/-	1°F
6	Power Supply	BK Precision	1710A 30B/1A	0-30 Volts	+/-	NA
NA	Pressure Calibrator	Beta	Beta Gauge PI PRO	NA	+/-	0.05% FS

Figure 6, Instrumentation Identification

A barometer was required for this experiment, because both differential pressure transducers reference atmospheric pressure. This allowed the pressure readings from the transducers to be standardized for calculations. The barometer that was used is a Conex Electro-Systems model JDB-1with a range of 9.8 to 15.2 psia and an uncertainty of +/- 0.025 psi. The barometer displayed 29.90 inches of mercury during the experiment, which is the local atmospheric pressure adjusted to seal level. The true atmospheric pressure at the elevation of Pocatello (4464 ft) is 12.50 psia. This pressure reading was checked with conditions at the Pocatello airport where the sea level adjusted atmospheric pressure was recorded as 30.67 inches of Mercury. At an elevation of 4,478 ft (Appendix E) the local atmospheric pressure is 12.86 psia. The difference between the two measurements could be due to elevation differences or a local high or low pressure region. The reading from the barometer along with its reported uncertainties will be used in the calculations.

A data acquisition system was used to collect the upstream temperature and pressure readings, along with the downstream temperature and pressure readings during the duration of the test. In this experiment, a Graphtec midi Logger GL820 was used. The data acquisition system (DAQ) recorded measurements every 250 ms without any filters. The settings are shown in Figure 7, in the header of the recorded data. The owner's manual reported a 0.1% uncertainty of the full scale voltage. For both transducers, a 50 Volt range was used. This means that the voltage uncertainty equals ± 0.05 volts. This correlates to ± 0.025 psi for the 25 psi differential pressure transducer (DPT), and ± 0.01084 psi for the 300 inches of water DPT. This does not take into account the uncertainty of the DPT itself.

Vendor	GRAPHTEC Corporation						
Model	GL820						
Version	Ver1.03						
Sampling interval	250ms						
Total data points	151						
Start time	11/17/2014	12:47:56					
End time	11/17/2014	12:48:34					
Trigger time	11/17/2014	12:47:56					
AMP settings							
CH	Signal name	Input	Range	Filter	Span		
CH1	P TANK	DC	50V	Off	-64.106	69.503	[psi]
CH2	P UPSTREAM	DC	50V	Off	149.5	-161.75	[psi]
CH3	T TANK	TEMP	TC_K	Off	3000	-200	[degF]
CH4	T UPSTREAM	TEMP	TC_K	Off	3000	-200	[degF]
Logic/Pulse	Off						
Data							
Number	Date&Time	ms	CH1	CH2	CH3	CH4	
NO.	Time	ms	psi	psi	degF	degF	
1	11/17/2014 12:47	0	-11.657	-3.07	65.5	67.5	
2	11/17/2014 12:47	250	-11.664	-3.07	65.7	67.5	

Figure 7, DAQ Output Data

The owner's manual of the DAQ also reported for a k-type thermocouple for the range of -100˚C < T < 1370˚C, the uncertainty is ± (0.05% of reading + 1.0) ˚C. The largest temperature reading was just above room temperature, which means that the uncertainty for the thermocouples were ± 1.0˚C or ± 1.8˚F. This does not take into account the uncertainty in the thermocouple itself.

Two differential pressure transducers were used to determine the upstream and downstream pressures. Both transducers referenced atmospheric pressure. The upstream pressure transducer had a range of 25 psid and the downstream pressure transducer had a range of 300 inches of water or 10.84 psi. These transducers were connected to the data acquisition system electrically.

The two DPTs that were used for this experiment were Omega Model-PX771A DPTs. The operation manual reported ± 0.15% of the upper range limit. The level of uncertainty for the 25 psid DPT is ± 0.0375 psi, and level of uncertainty for the 300 inches of water DPT is ± 0.01626 psi. This does not take into account the uncertainty in the DAQ for the DPTs.

A pressure calibrator was used to calibrate the DPTs. A Beta Gauge PI PRO calibrator with a +/- 0.05% FS, was connected with a pressure tube fitting to each DPT. The pressure calibrator had a hand pressure pump with a digital display. The calibrator would display the pressure regardless if the hand pump was used or not. The DAQ displayed the DPTs pressure reading, which was then compared to the pressure calibrator reading. This process verified that the DPTs and the DAQ for the pressure measurements were calibrated and producing accurate readings. The calibration procedure is discussed in Appendix B.

With the DPTs calibrated, the uncertainty for DPTs was assumed to be the uncertainty of the pressure calibrator. The uncertainty for the 25 psid DPT is considered to be ± 0.0125 psi, and the uncertainty for the 300 inches of water DPT is considered to be ± 0.00542 psi.

To find the total uncertainty on the pressure readings, the uncertainty of the DAQ, barometer, and the DPT must be combined into a total uncertainty. The total uncertainty for the pressure readings is calculated by taking the square root of the sum of squares, which is shown in Table 5.

A power source of at least 8 volts must be supplied to the differential pressure transducers in order to power them up. The power supply used is a BK Precision model number 1710A 30B/1A with a 0-30 volt range.

Two k-type thermocouples were used to determine the upstream and downstream temperatures of the nitrogen during the test duration. These thermocouples were connected to the data acquisition system. The thermocouples were produced at Idaho Laboratories, located in Idaho Falls, and were designed for a Swagelok fitting that allows the thermocouple to slide in as far as needed.

The thermocouple manufacturer reported, for the range of 32˚F to 100˚F, an uncertainty of +/- 1˚F. The experiment stays well within this temperature range. This uncertainty does not take into account the uncertainty in the DAQ for the thermocouples. The total uncertainty for the temperature readings is calculated by taking the square root of the sum of squares, which is also shown in Table 5.

Table 5, Pressure and Temperature Uncertainties

Pressure & Temperature Uncertainties				
300 inch DPT	Barameter	+/-	0.025	psi
	DAQ	+/-	0.01084	psi
	DPT	+/-	0.00542	psi
	Total Uncertainty	**+/-**	**0.02778**	**psi**
25 psi DPT	Barameter	+/-	0.025	psi
	DAQ	+/-	0.025	psi
	DPT	+/-	0.0125	psi
	Total Uncertainty	**+/-**	**0.0375**	**psi**
Thermo-couples	DAQ	+/-	1.8	°F
	Thermocouple	+/-	1	°F
	Total Uncertainty	**+/-**	**2.06**	**°F**

Chapter V: Setup and Test Procedure

Test Setup

This section includes information on how the experimental apparatus was setup. It details how each piece of equipment connects to surrounding equipment either by electrical connections or by piping or fittings. The experimental apparatus, as shown in Figure 8, was assembled in the Idaho State University's fluid and thermodynamics laboratory.

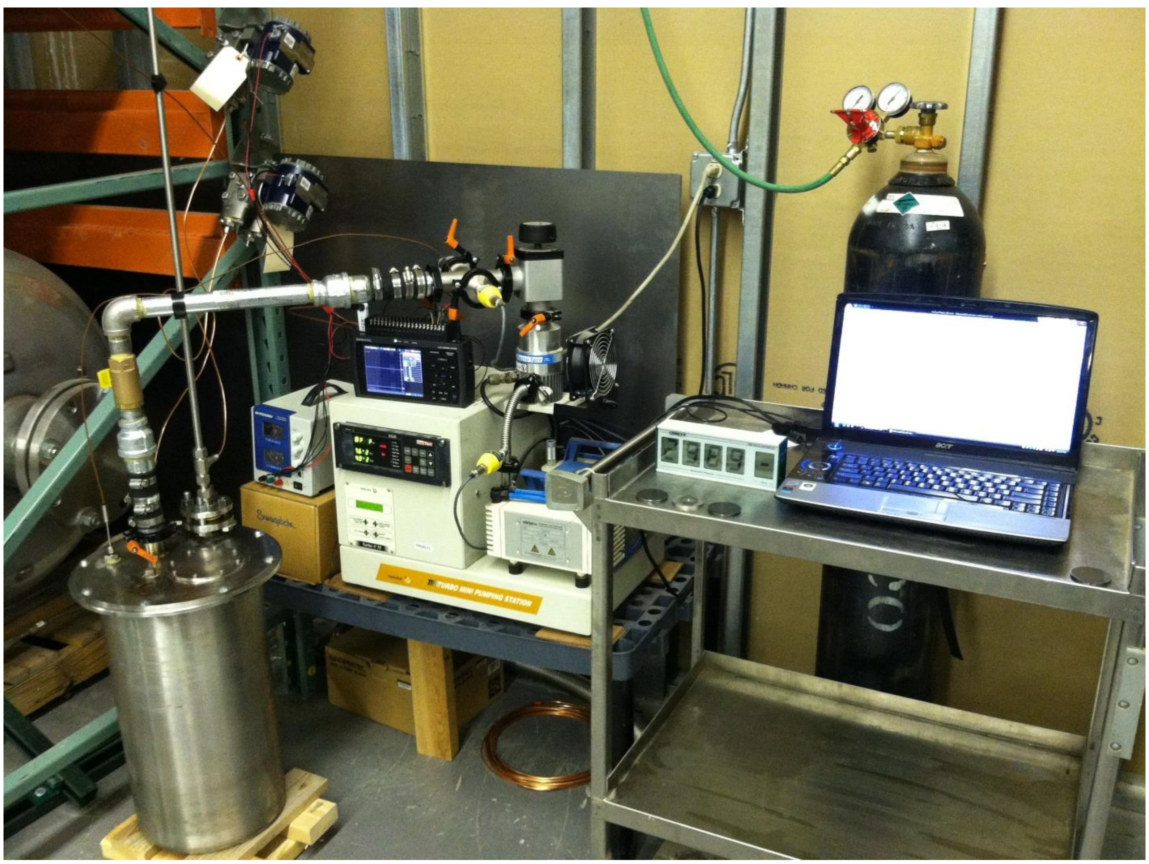

Figure 8, Experimental Apparatus

The function of the DAQ was to take voltage measurements from the thermocouples and DPTs and then translate that into temperature and pressure readings. The DAQ contains channel terminals. Each channel terminal consists of a positive and negative terminal. The instrumentation was connected to the DAQ terminals per the DAQ requirements (see Figure 9 or to the Omega differential pressure transducer wiring diagram as located in the Appendix E).

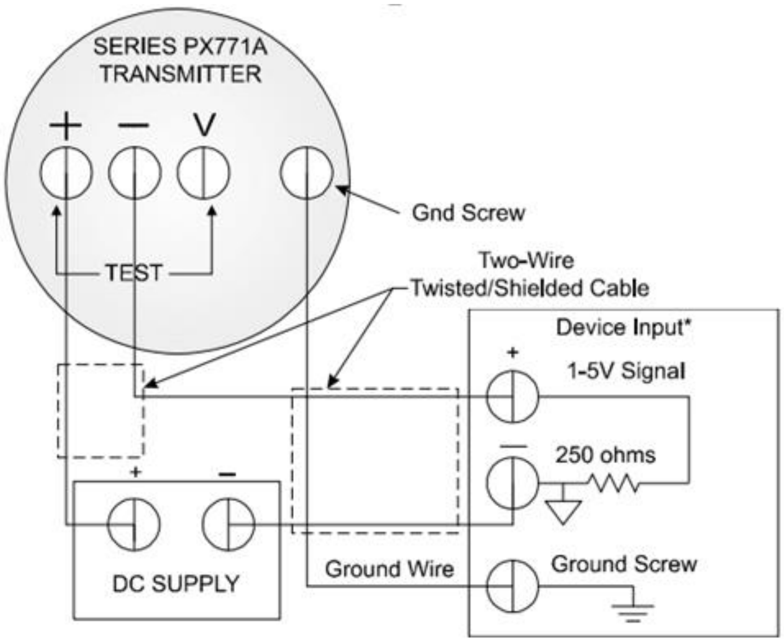

Figure 9, DPT wiring to DAQ

The wiring diagram indicates that a 250 ohm resistor is to be placed between the positive and negative terminals on the DAQ for the DPTs, thus forming a 250 ohm resistance bridge between the two terminals. Photographs of the wiring connections are given in Figure 10.

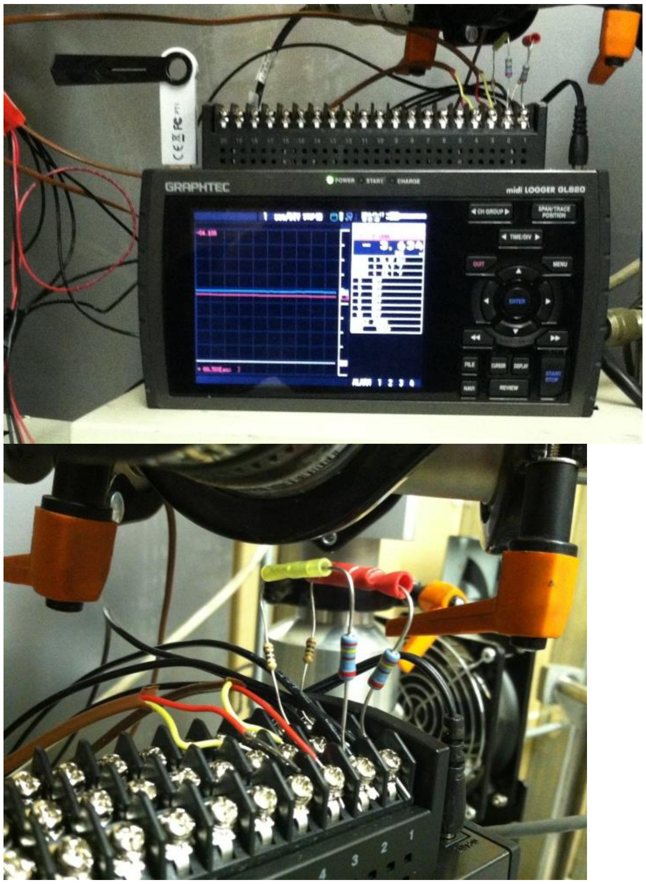

Figure 10, DAQ wiring

The manual for the DAQ instructs the user on how to properly setup a thermocouple and DPT to the DAQ. The DAQ has factory settings for varying thermocouple types, and only requires a simple setting change to accommodate the k-type thermocouple. The setup of the DPT to the DAQ, is more complicated. Each DPT has a working range. For instance, the upstream DPT has a pressure range of 0 to 25 psid, and a voltage range of 1 to 5 volts. This means that if the DAQ is reading 1 volt, then the pressure is 0 psid, or if the DAQ is reading 5 volts, then the pressure is 25 psid. The DPT response is linear between these end points. This allows the DAQ to use these upper and lower limits to convert a voltage measurement into a pressure reading.

The DPTs each have two pressure ports and four electrical terminals. They have a high and low pressure port which allows only one direction of movement. The upstream DPT high pressure port was connected to the upstream line. It was decided to have the low pressure port reference atmospheric pressure, so no connection on this port was necessary. The downstream DPT low pressure port was connected to the receiving tank, because the tank experienced negative gage pressures. The high pressure port referenced atmospheric pressure, so no connection on this port was necessary. Teflon tape or pipe dope should was used on the threads of these fittings to prevent leaks. The DPT to DAQ calibration process is discussed in Appendix B.

The DPT electrical terminal consists of a ground, negative, positive, and a V terminal. It both connects to the DAQ and power supply, as shown in Figure 9. To see full diagram and wiring instructions, refer to the Omega DPT wiring diagram in Appendix E. A photograph of the wiring and connections for the DPTs can be seen in Figure 11.

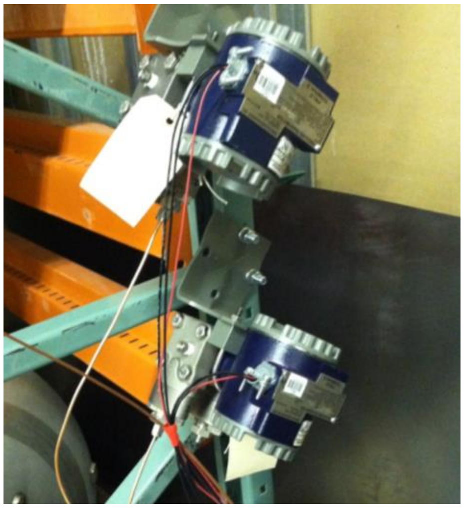

Figure 11, DPTs wiring and connections

The entrance line to the orifice plate must house a thermocouple and a pressure tap fitting. The thermocouple was placed far enough away from the orifice plate, so as to not cause flow disturbance near the orifice. A Swagelok tee fitting was used for both the thermocouple and pressure tap. The thermocouple was placed 4 feet upstream of the orifice plate, and the pressure tap fitting was placed 3.5 inches upstream of the orifice plate. The entrance line to the receiver tank can be seen in Figure 12.

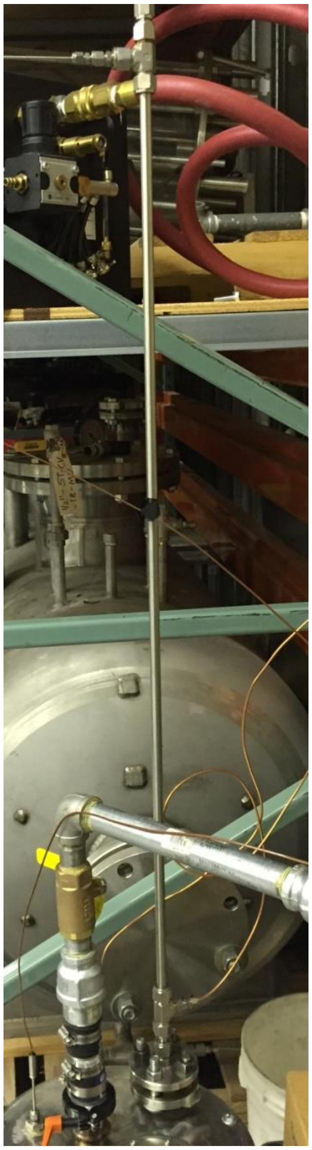

Figure 12, Entrance Line

The orifice plates were located between the entrance line and receiver tank in a bolt flange fitting. The bolt flange fitting consisted of two heavy duty flanges with a bolt pattern and sealing gaskets. The orifice plate was placed between sealing gaskets, which was centered in between the two flanges. The bolts tightened the two flanges together, thus sealing the flange to the seals and the seals to the orifice plate. By using a bolt flange, it allows an orifice plate to be removed and installed again with little effort. This setup is shown in Figure 13.

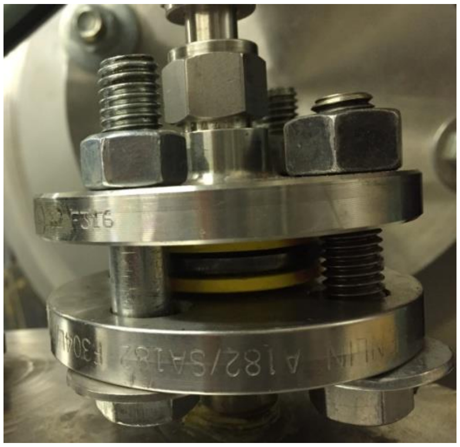

Figure 13, Orifice plate setup

The DPTs call for an excitation voltage somewhere between 8 and 24 volts. It was decided to use 10 volts to excite or power up the DPTs. The power supply was connected to the DPTs and DAQ as required by the equipment specifications, as shown in Figure 9, or in the Omega differential pressure transducer wiring diagram given in Appendix E. A photograph of the power supply is shown in Figure 14.

Figure 14, Power supply wiring

Two thermocouples were used for this experiment, one for the upstream line, and the other for the receiver tank. Both thermocouples were designed for a Swagelok fitting that allowed the thermocouple to slide in as far as needed and then lock and seal into place. The thermocouple wire connections to the DAQ, are shown in Figure 10.

Two different types of leak tests were performed on the experimental apparatus, and descriptions of both are given in Appendix B. The leak tests confirmed the experimental apparatus to be leak free.

Test Procedure

The test procedure used for these experiments follows:

(1) Before attaching nitrogen bottle to the upstream line, the nitrogen valve was opened and the regulator pressure was set to 20 psig. Next, the nitrogen valve was closed and the pressure regulator was attached to the upstream line.

(2) The desired orifice plate was placed in the flange with the orifice hole centered in the flange line, and then the flange retaining bolts were tightened.

(3) A leak test was performed to ensure that no leaks were present. Refer to Appendix B for leak testing procedures.

(4) The valve located between the receiver tank and vacuum pump was opened.

(5) The vacuum pump was turned-on and the pump depressurized the receiver tank to the minimum level achievable with this hardware configuration. Refer to the Description of Hardware section for this vacuum pressure.

(6) The valve located between the receiver tank and vacuum pump was closed.

(7) To further reduce the quantity of air in the receiver tank, the nitrogen valve was opened and nitrogen was allowed to enter the receiver tank. The nitrogen valve was turned off when the receiver tank pressure reached around 0 psig.

(8) The vacuum line valve was slowly opened. The valve must be opened slowly, so as to not damage the turbo blades in the vacuum pump.

(9) The vacuum pump was turned-on and the receiver tank was depressurized to the minimum pressure level a second time to minimize the quantities of gas components that are not nitrogen. The vacuum line valve was closed.

(10) The data acquisition system was initiated and began to record data.

(11) The nitrogen bottle valve was opened and nitrogen began to flow through the orifice plate and into the receiver tank.

(12) Once the receiver tank pressure was 0 psig (the DPTs range limit), the data acquisition system recorder was switched off.

(13) The test run was completed when the nitrogen bottle valve was closed.

(14) If another test run was to be performed, the vacuum line valve was slowly opened. The valve must be opened slowly, so as to not damage the turbo blades in the vacuum pump.

(15) Repeat steps 2-14 to test the next orifice plate.

Chapter VI: Methodology

The main reasons for using a critical flow orifice to measure mass flow are simplicity, low cost, and quick turnaround:

(A) Simplicity: mass flow can be measured by knowing only the fluid properties, the thermodynamic state upstream of the orifice, and the geometry of the orifice and upstream piping. The downstream pressure does not affect the measurement if the orifice is choked.

(B) Low Cost: an orifice plate and the upstream piping can be constructed and assembled at almost the lowest cost of any flow measuring instrumentation.

(C) Quick Turnaround: A critical orifice plate can quickly be constructed.

Zucker Equation

By using compressible fluid flow techniques and equations, the mass flow rate can be determined. Taking Zucker and Biblarz's equations, Reference 15

Equation 1, Mach Number

$$M = \frac{V}{a}$$

Equation 2, Speed of Sound

$$a = \sqrt{\gamma R T}$$

Equation 3, Mass Flow Rate

$$\dot{m} = \rho V A$$

Equation 4, Ideal Gas

$$\rho = \frac{P}{RT}$$

and combining, simplifying, and solving for the mass flow rate results in

Equation 5, Ideal Mass Flow Rate

$$\dot{m} = PAM\sqrt{\frac{\gamma}{RT}}$$

where $\dot{m}$ is the mass flow rate, P is the pressure, A is the area of the orifice, M is the mach number at the orifice (M=1 for choked flow), γ is the specific heat ratio, R is the gas constant, and T is the temperature. Equation 5 assumes that nitrogen is a perfect gas and that the conditions (temperature and pressure) are at the location where the Mach number is 1. In order to use this equation, the temperature and pressure at the throat of the orifice are required. And therefore Equation 5 is impractical to use in most application—and will not be used in this application.

A similar equation that assumes the Mach number is 1, but that the temperature and pressure is known as a stagnation upstream condition is

Equation 6, Zucker's Critical Mass Flow Rate[1]

$$\dot{m} = \frac{AP_t}{\sqrt{T_t}}\left[\frac{\gamma}{R}\left(\frac{2}{\gamma + 1}\right)^{\frac{\gamma+1}{\gamma-1}}\right]^{\frac{1}{2}}$$

where P_t is the upstream stagnation pressure, and T_t is the upstream stagnation temperature. This equation can be found in Zucker and Biblarz, 2002, equation 5.44b. It has been found that in order to render accurate results with this equation, a discharge coefficient must be used. Rearranging, manipulating, and adding a discharge coefficient to Equation 6 results in

[1] This equation is taken from Zucker and Biblarz, 2002 and will be identified in this thesis as the Zucker equation.

Equation 7, Zucker's Critical Mass Flow Rate with Discharge Coefficient

$$\dot{m} = C_d A \left[\gamma \rho P_t \left(\frac{2}{\gamma + 1} \right)^{\frac{\gamma+1}{\gamma-1}} \right]^{\frac{1}{2}}$$

where C_d is the discharge coefficient, and ρ is the upstream stagnation density. Reference 6 states that for a sharp edge orifice

$$C_d = 0.839 \quad if \quad 1 < \frac{t}{d} < 10$$

where t is the thickness of the orifice plate, and d is the diameter of the orifice. If this discharge coefficient, the area equation of the orifice, and the specific heat ratio of nitrogen is substituted into Equation 7 and then simplified, results in

Equation 8, Zucker's Critical Mass Flow Rate Simplified

$$\dot{m} = (0.451203) d^2 \sqrt{\rho P_t}$$

where d is the diameter of the orifice. This equation is only valid for nitrogen and an orifice plate that meets the above mentioned criteria.

Zucker's equations use stagnation conditions verses static conditions. A correctional factor, given by R.W. Miller, 1983 (Reference 16), may be applied to transform the measured static pressure to total pressure

$$P_t = \left[1 + \frac{\gamma}{2} \left(\frac{2}{\gamma + 1} \right)^{\frac{\gamma+1}{\gamma-1}} * \left(\frac{d}{D} \right)^4 \right] * P_s$$

where P_s is the static pressure, and P_t is the total pressure. The correctional factor was applied to Spink's equation and found to have negligible effect on the calculated results.

Spink Equation

Another method to determine the mass flow rate through the orifice is to use L.K. Spink's equation (Reference 14, equation 56)

Equation 9, Spink's Critical Mass Flow Rate

$$W_h = 359\, Y_T S_P D^2 F_a \sqrt{\gamma_{f1}} \sqrt{p_{f1}}$$

where W_h is the hourly rate of flow in pounds, Y_T is the expansion factor at the critical pressure ratio for throttling orifices, S_P is the $K_0\beta^2$ for full-flow taps, K_0 is the coefficient of discharge including the velocity of approach, i.e., the flow coefficient, β is the ratio of the orifice throat diameter to the diameter of the upstream pipe, D is the actual inside diameter of the pipe, F_a is the factor for temperature expansion of the orifice, γ_{f1} is the specific weight for the flowing fluid at upstream conditions in pounds per cubic foot, and p_{f1} is the upstream static pressure in psia. $Y_T S_P$ can be found using Figure B-2525 (Reference 14 or Appendix E) as an approximation of air, or using this equation (Reference 14, equation 53)

Equation 10, Spink's YtSp

$$Y_T S_P = \frac{W_h}{4.81 D^2 F_a F_{tf} F_{pv} p_{f1} \sqrt{m_w}}$$

where $Y_T S_P$ is the combined factor, F_{tf} is the flowing temperature factor, F_{pv} is the supercompressiblity factor, and m_w is the molecular weight.

When using Figure B-2525, $Y_T S_P$ is found by using a d/D ratio where d is the orifice diameter and D is the entrance line diameter. Figure B-2525 shows a minimum d/D value of 0.10. This means that the graph must be extrapolated to find $Y_T S_P$ for the 1/32-inch and 1/64-inch orifice plates. Values of $Y_T S_P$ and d/D were placed in excel from

Figure B-2525 to produce a power function trend line equation (extrapolation equation) and graph, as shown in Figure 15.

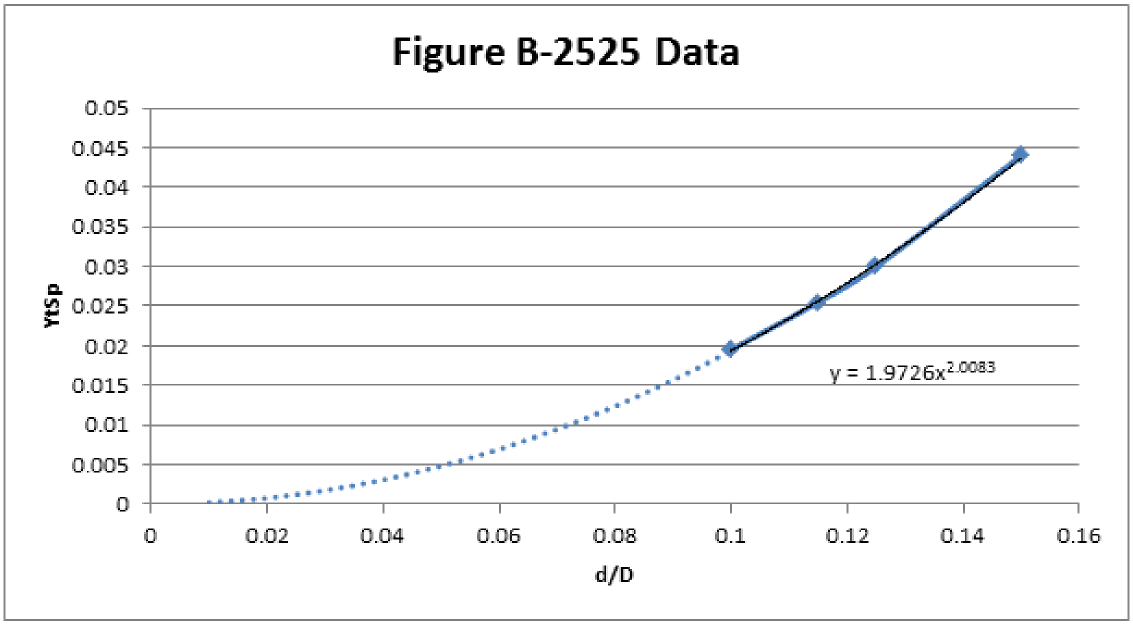

Figure 15, YtSp Trendline Graph

Using the displayed equation in Figure 15, $Y_T S_P$ was calculated and is shown in Table 6. This same equation was substituted into Equation 9. This would allow the results to be calculated without having to look up a new $Y_T S_P$ value for a differing orifice size.

Table 6, Extrapolated YtSp value for the 1/32-inch & 1/64-inch

Orifice Size	d/D	YtSp
1/32-inch	0.073	0.0102
1/64-inch	0.037	0.0027

Discussion of Differences Between Zucker and Spink Equations

The Zucker and Spink equations are surprisingly different and thus should be examined to identify the correspondence between terms. To accomplish this task, because both equations calculate the critical flow through an orifice plate, the two equations are set equal to one another while adding a δ to the right-hand-side to represent the quantitative difference between the two equations. If the two equations are identically equal then the residue, when evaluated, will be identically equal. If the two equations are not identically equal then the two sides can be compared to establish the ratio be one to the other. The unlike terms are then examined one-by-one.

To simplify the comparison the form of the Zucker equation given in Miller is used to compare to the Spink equation where the two equations are cast in a form where the same units are used for the primary variables, i.e., the units of static pressure (P_s) are lbf/in^2, the units of density (ρ) are lbm/ft^3, the units of mass flow rate ($\dot{m}$) are lbm/s, and the units of diameter (d or D) are in^2. In the following expression the Zucker equation is placed on the left and the Spink equation on the right:

$$0.3712458 C d^2 \sqrt{Z_f} Y_{CR} \sqrt{\rho} \sqrt{F_{TP}} \sqrt{P_s} = 0.09972222 Y_T S_P D^2 F_a \sqrt{\rho} \sqrt{P_s} + \delta$$

where for the example given here, the gas is nitrogen, the orifice diameter is 1/16-inch, the upstream pipe inner diameter is 0.4301 inch, and the ratio of specific heats for nitrogen is 1.4:

d = diameter of orifice (inches) = 1/16 inch = 0.0625 inch

D = diameter of the piping upstream of the orifice (inches) = 0.4301 inch

β = d/D = ratio of the orifice diameter to the upstream piping diameter = 0.1453

C = discharge coefficient for orifice = 0.83932

Z_f = compressibility factor

k = ratio of specific heats = 1.4 for nitrogen

$Y_{CR} = \left[\frac{k}{Z_f}\left(\frac{2}{k+1}\right)^{\frac{k+1}{k-1}}\right]^{1/2} = \left[\frac{0.4689}{Z_f}\right]^{1/2}$

ρ = density of nitrogen (lbm/ft^3)

$F_{TP} = \left[1 + \frac{k}{2}\left(\frac{2}{k+1}\right)^{\frac{k+1}{k-1}}\beta^4\right]$

P_s = static pressure upstream of orifice (lbf/in^2)

Y_T = expansion factor for throttling orifices at 50% pressure drop

$S_P = K_o\beta^2$ for full-flow taps

$Y_T S_P = 1.942\beta^2$ based on Figure B-2525 of Spink

F_a = factor for temperature expansion of the orifice plate = 1. @ 80 °F

δ = difference between the two equations (lbm/s)

The constant given on the left hand side of the Zucker equation = 0.3712458 is a composite of the conversion factors necessary to assure unit consistency as well as to include necessary constants such as $\pi/4$ and equals $\frac{\pi}{4}\left[\frac{32.2}{144}\right]^{1/2} = 0.3712458$. The constant given on the left hand side of the Spink equation = 0.09972222 serves a similar purpose.

Canceling like terms on the right and left sides of the above equation and inserting constants and defining expressions given above, the above equation becomes:

$$0.3712458(0.83932)(0.0625)^2(0.4689)^{1/2}[1 + 0.2344(0.1453)^4]^{1/2}$$

$$= 0.09972222[1.942(0.1453)^2](0.4301)^2 + \acute{\delta}$$

or

$0.00083351 = 0.00075633 + \acute{\delta}$ or $\acute{\delta} = 0.00007718$

The above shows that the Zucker equation will always predict a larger mass flow rate than the Spink equation. The differences between the two equations stem from the simplifications included in the Spink equation as well as the use of an empirical approach for estimating what is in effect the discharge coefficient based on the geometry of the orifice meter coupled with ratio of the approach pipe inner diameter to the orifice diameter. In addition, two observations are important: (i) The estimate of the product of the expansion factor for throttling orifices at 50% pressure drop and factor for using full-flow taps, shown in Figure 15, required a trend-line approximation for the 1/32-inch and 1/64-inch diameter orifices and (ii) the approach outlined in Spink predates the work done by Ward-Smith described earlier and recorded in Miller. These differences combine to render the Spink approach to be less accurate than the Zucker equation.

Experimentally-Measured Mass Flow

Equations 5, 7, and 9 indicate that the testing apparatus must measure upstream pressure and temperature. Therefore a thermocouple and differential pressure transducer port were placed in the upstream line to continually monitor the temperatures and pressures with time, as noted in Chapter IV.

The equations used to calculate the predicted mass flow rate require the diameter of the orifice. The diameter of the orifice can be approximated by using the diameter size of the drill bit that drilled the orifice. However, the actual orifice size will most likely be larger than the drill bit size due to drill bit over sizing and drill bit wobble. The area of the orifice is calculated by

Equation 11, Area of a Circle

$$A = \frac{\pi}{4} D^2$$

where A is the area of the orifice, and D is the diameter of the orifice. The equation can be rearranged to

Equation 12, Area of a Circle Rearranged

$$D = \sqrt{\frac{4A}{\pi}}$$

which if the actual area can be determine by some method, then a correctional diameter can be solved for and then inserted into the mass flow rate equations to render a more accurate calculation. One method used to more accurately determine the area of an object is by counting digital pixels. This method is described in Appendix A.

The next mathematical step in this process is to find an equation that will solve for the actual mass flow rate. This flow rate is determined by the nitrogen that leaves the orifice plate and gathers in the receiver tank. There must be a way to determine how much mass is actually in the receiver tank, or how the mass in the receiver tank is changing with time. Combining these two equations

Equation 13, Mass

$$m = \rho \forall$$

Equation 4, Ideal Gas

$$\rho = \frac{P}{RT}$$

and solving for m results in

Equation 14, Mass using Ideal Gas

$$m = \frac{P \forall}{RT}$$

where m is the mass, P is the pressure, ∀ is the volume of the receiver tank, R is the gas constant, and T is the temperature of the gas. To find the mass flow rate use

Equation 15, Mass Rate

$$\dot{m} = \frac{\Delta m}{\Delta t}$$

or

Equation 16, Mass Flow Rate for Constant Volume

$$\dot{m} = \frac{\frac{\forall}{R}\left(\frac{P_2}{T_2} - \frac{P_1}{T_1}\right)}{t_2 - t_1}$$

where t is the time, and subscript 1 is the condition at state 1, and subscript 2 is the condition at state 2. The volume and gas constant variables remain constant between state 1 and state 2. This is why the volume and gas constant variables are factored outside of the equation. This equation was formed by using the ideal gas equation, thus it assumes that nitrogen is an ideal gas. To render a more accurate result, an equation of state tailored for nitrogen could be used.

The Benedict-Webb-Rubin equation 3-26 (Reference 17), is an equation better tailored for nitrogen,

Equation 17, Benedict-Webb-Rubin

$$P = \frac{R_u T}{\bar{v}} + \left(B_0 R_u T - A_0 - \frac{C_0}{T^2}\right)\frac{1}{\bar{v}^2} + \frac{b R_u T - a}{\bar{v}^3} + \frac{a\alpha}{\bar{v}^6} + \frac{c}{\bar{v}^3 T^2}\left(1 + \frac{\gamma}{\bar{v}^2}\right) e^{-\gamma/\bar{v}^2}$$

where P is the pressure, R_u is the universal gas constant, T is the temperature, $\bar{v}$ is the specific volume per unit mole, and the rest of the variables are constants for nitrogen that can be found in Table 3-4(b) of Reference 17. Example problem 3-13 compares the Benedict-Webb-Rubin equation to experimental data of nitrogen at 10,000 kPa and at 175

K. It places this equation with a 0.09 percent error, which it states, "… is rather impressive…"

The Benedict-Webb-Rubin equation does an excellent job of predicting gas behavior when the gas is at extreme or critical conditions. The ideal gas equation is unable to produce accurate results when this is the case. The ideal gas equation solutions were compared with the Benedict-Webb-Rubin equation solutions for this experiment. It was found that both equations produced the same results with minimal deviation. This is because the nitrogen remains near room temperature conditions. For simplicity, the ideal gas equation will be used to calculate the upstream and downstream conditions in place of the Benedict-Webb-Rubin equation.

An investigation of uncertainty produced by using the ideal gas equation also was taken into account. A compressibility factor is often assigned to the ideal gas equation for a specific gas and operating condition. The compressibility factor converges to one as the pressure approaches zero gage pressure. Thus the ideal gas equation has a minimal, and for the purposes of this research, negligible uncertainty. Therefore the ideal gas equation will be used to calculate the upstream and downstream conditions in place of the Benedict-Webb-Rubin equation or by using a compressibility factor.

Equations 14 and 16 indicate that in order to calculate the mass in the tank, the testing apparatus must measure the receiver tank temperature and pressure. A thermocouple and differential pressure transducer port was placed in the receiver tank to continually monitor the tanks temperature and pressure with time.

The equations also indicate that the volume downstream of the orifice plate must be known in order to calculate the mass flow rate. The volume downstream of the orifice plate consists of the receiver tank, the vacuum line, the pressure line to the DPT, and the volume in the DPT. To calculate the downstream volume using geometry and measurements would be time consuming and not very accurate. A more accurate method to determine the volume downstream of the orifice plate is to use a liquid such as water. Water can be added to the receiver tank, vacuum line, pressure line, and the DPT, and then the volume of the water can be measured using graduated cylinders. This process can be found in Appendix A.

Measurement and Calculational Uncertainties

Equations 5, 7, and 9 all assume that no errors or uncertainties reside in the variables. All measurements and instruments produce errors, so an uncertainty interval must be developed to model these errors. The ASME national standard for computing the measurement uncertainty of fluid flow in a closed conduit (Reference 18) describes the procedure to correctly capture uncertainties in flow calculations and is used to compute the measurement uncertainty for both the experiment and the calculations in this thesis. The ASME national standard states:

> Uncertainty is a function of the measurement process. It provides an estimate of the error band within which the true value for that measurement process must fall with high probability. Errors larger than the uncertainty should rarely occur. On repeated runs within a given measurement process, the parameter values should be within the uncertainty interval. Run-to-run differences between corresponding values of the parameter should be less than the uncertainty for the parameter.

The standard then describes how the errors in the measurements are propagated through the function, and how this effect can be approximated by using a Taylor series expansion method. The standard gives an example problem demonstrating this technique for a choked venturi.

Using Reference 18, the Taylor series expansion equation was tailored for Equation 7,

Equation 18, Taylor Series Expansion Tailored for Eq. 7

$$S_m = \sqrt{\left(\frac{\partial_m}{\partial_d} S_d\right)^2 + \left(\frac{\partial_m}{\partial_P} S_P\right)^2 + \left(\frac{\partial_m}{\partial_T} S_T\right)^2}$$

where S_m is the mass flow rate precision index, d is the orifice diameter and S_d is its precision index, P is the upstream pressure and S_P is its precision index, and T is the upstream temperature and S_T is its precision index. Notice that the density is not included in equation 18 since it is a direct function of the fluid pressure and temperature via the ideal gas law. Also, as noted in the ASME national standard, the uncertainties of both the ratio of specific heats and the compressibility are both negligible when evaluated at the proper thermodynamic conditions (see Reference 18, Section 2.3.2.4, page 41). The precision index equation was similarly tailored for Equation 9

Equation 19, Taylor Series Expansion Tailored for Eq. 9

$$S_m = \sqrt{\left(\frac{\partial_m}{\partial_d} S_d\right)^2 + \left(\frac{\partial_m}{\partial_P} S_P\right)^2 + \left(\frac{\partial_m}{\partial_T} S_T\right)^2}$$

where S_m is the mass flow rate precision index, d is the orifice diameter and S_d is its precision index, P is the upstream pressure and S_P is its precision index, and T is the upstream temperature and S_T is its precision index.

The precision index equation tailored for Equation 16 is

Equation 20, Taylor Series Expansion Tailored for Eq. 16

$$S_m = \sqrt{\left(\frac{\partial_m}{\partial_V} S_V\right)^2 + \left(\frac{\partial_m}{\partial_P} S_P\right)^2 + \left(\frac{\partial_m}{\partial_T} S_T\right)^2}$$

where S_m is the mass precision index, V is the receiver tank volume and S_V is its precision index, P is the upstream pressure and S_P is its precision index, and T is the upstream temperature and S_T is its precision index.

After computing the partial derivatives and applying the constant values, Equation 7 becomes

$$S_m = \sqrt{\left(0.814337 \frac{d^2 * P^2 * {S_d}^2}{R * T}\right) + \left(0.203584 \frac{d^4 * {S_P}^2}{R * T}\right) + \left(0.0508961 \frac{d^4 * P^2 * {S_T}^2}{R * T^3}\right)}$$

Equation 9 becomes

$$S_m = \left[\begin{array}{c} \left(5.3556 * 10^6 * d^{2.0166} * P * {S_d}^2 * \left(\frac{P}{T}\right)\right) + \\ {S_P}^2 \left(\left(576.164 \frac{d^{2.0083} * \left(\frac{P}{T}\right)^{0.5}}{P^{0.5}}\right) + \left(576.164 \frac{d^{2.0083} * P^{0.5}}{\left(\frac{P}{T}\right)^{0.5} * T}\right)\right)^2 + \\ \left(331965 \frac{P^3 * d^{4.0166} * {S_T}^2}{T^4 * \left(\frac{P}{T}\right)}\right) \end{array} \right]^{\frac{1}{2}}$$

and Equation 16 becomes

$$S_m = \left[\left(\frac{S_V^2 * \left(\frac{P_2}{T_2} - \frac{P_1}{T_1}\right)^2}{R^2 * (t_2 - t_1)^2}\right) + \left(\frac{V^2 * S_P^2}{R^2 * T_1^2 * (t_2 - t_1)^2}\right) + \left(\frac{V^2 * S_P^2}{R^2 * T_2^2 * (t_2 - t_1)^2}\right) + \left(\frac{P_1^2 * S_T^2 * V^2}{R^2 * T_1^4 * (t_2 - t_1)^2}\right) + \left(\frac{P_2^2 * S_T^2 * V^2}{R^2 * T_2^4 * (t_2 - t_1)^2}\right)\right]^{\frac{1}{2}}$$

The uncertainties associated with the temperature, pressure, orifice diameter, and receiver tank measurements are listed in the Hardware and Instrumentation sections and are also summarized below on Table 7.

Table 7, Precision Index/Uncertainty Summary

Precision Index Summary					
Orifice Diameter	1/16-inch	S_D	+/-	0.0625	in
	1/32-inch			0.03125	in
	1/64-inch			0.015625	in
DPT, DAQ & Barometer for Pressure	300 inch H_20	S_P	+/-	0.02778	psi
	25 psid			0.0375	psi
DPT & DAQ for Temperature	K-type thermocouple	S_T	+/-	2.06	°F
Receiver Tank Volume		S_V	+/-	0.00988	ft^3

Chapter VII: Results

The experiment, as explained in the Test Procedure section, consisted of four separate tests with four different orifice plates. The orifice sizes that were used were a 1/16-inch orifice, a 1/32-inch orifice, a 1/64-inch (#78) orifice, and a 1/64-inch (#78) orifice with an exit chamfer. Each test was run with an upstream pressure between 18 psig and 20 psig. During the duration of the test, the downstream pressure was initially around 1 psia and then increased to 13 psia at the end of the test.

The mass flow rate was calculated using Zucker (Equation 7), Spink (Equation 9), and the ideal tank equation (Equation 16). The results are shown on the graphs below, see Figures 15, 16, 17, and 18. Each orifice plate graph compares the mass flow verses time for each of the three equations. A second graph plots the upstream pressure during the duration of the test.

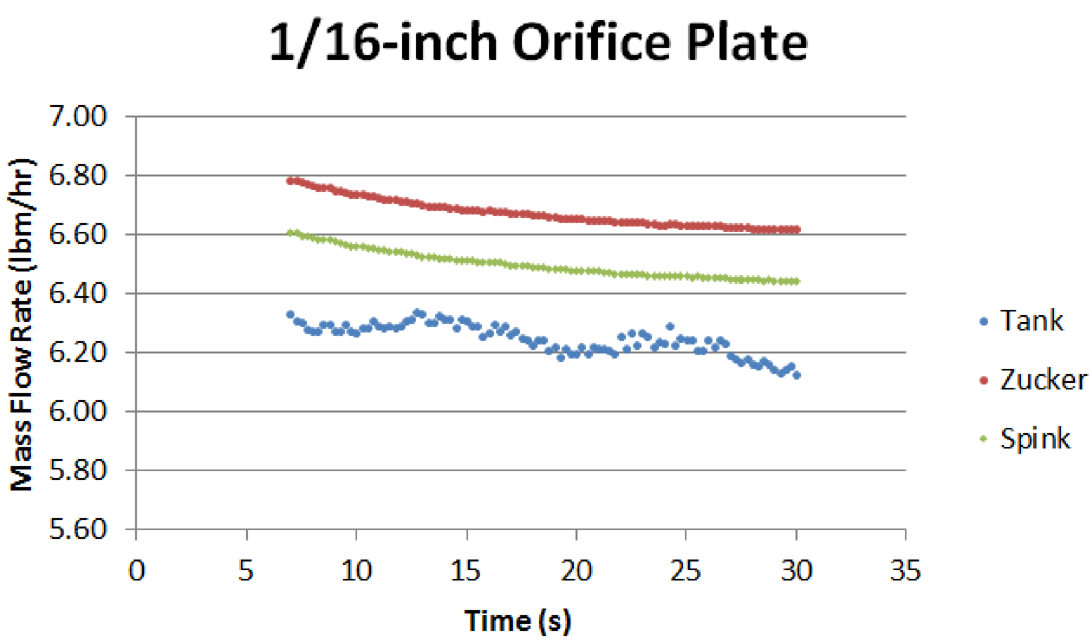

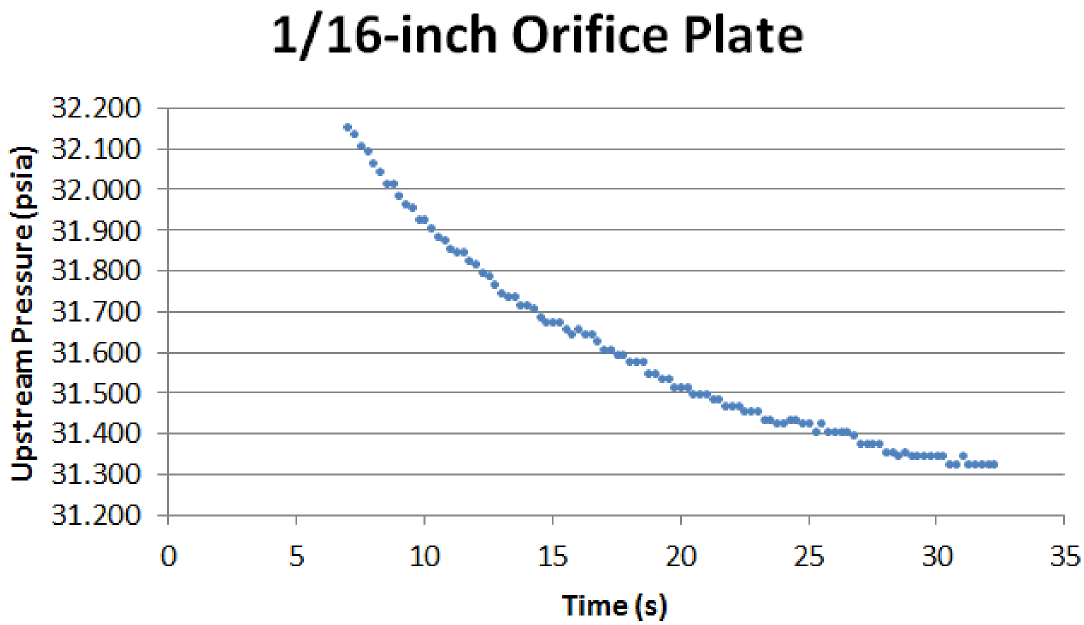

Figure 16, 1/16-inch Orifice Plate Test Graphs

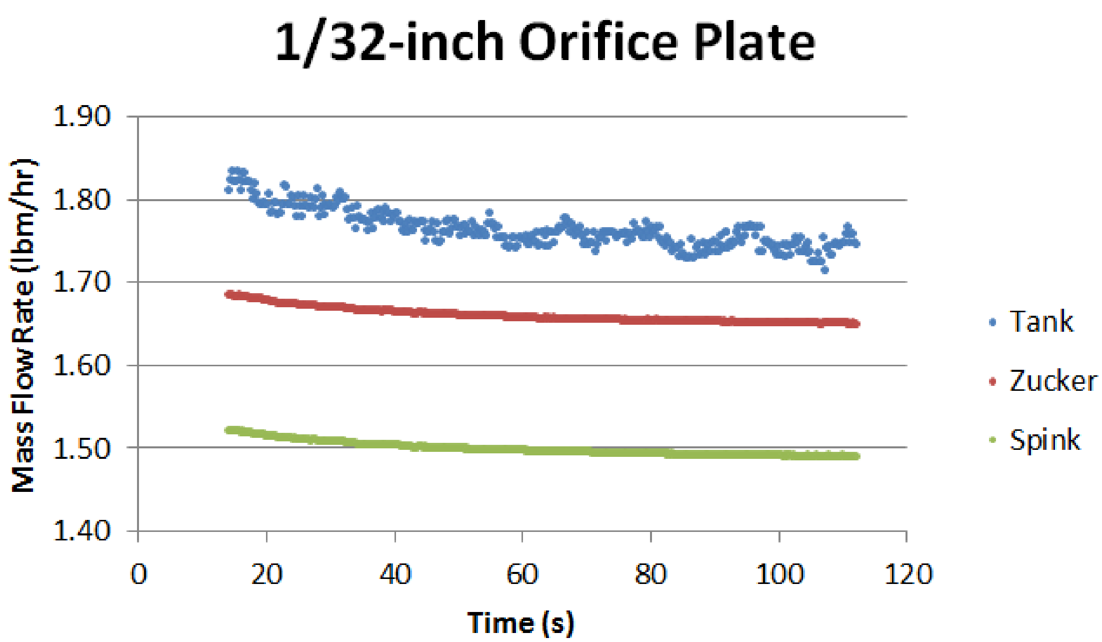

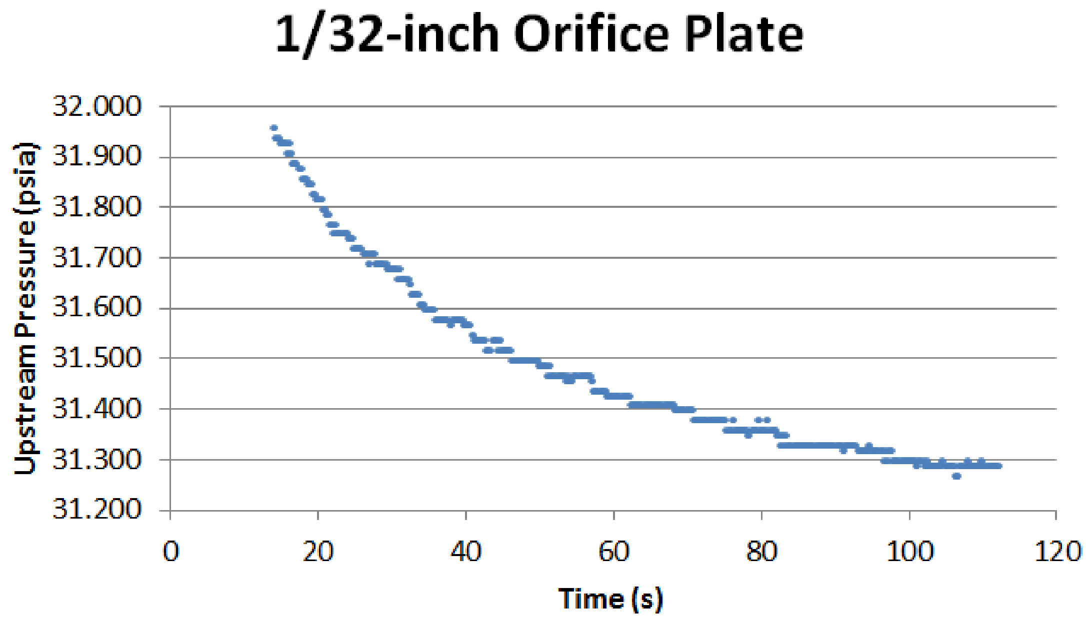

Figure 17, 1/32-inch Orifice Plate Test Graphs

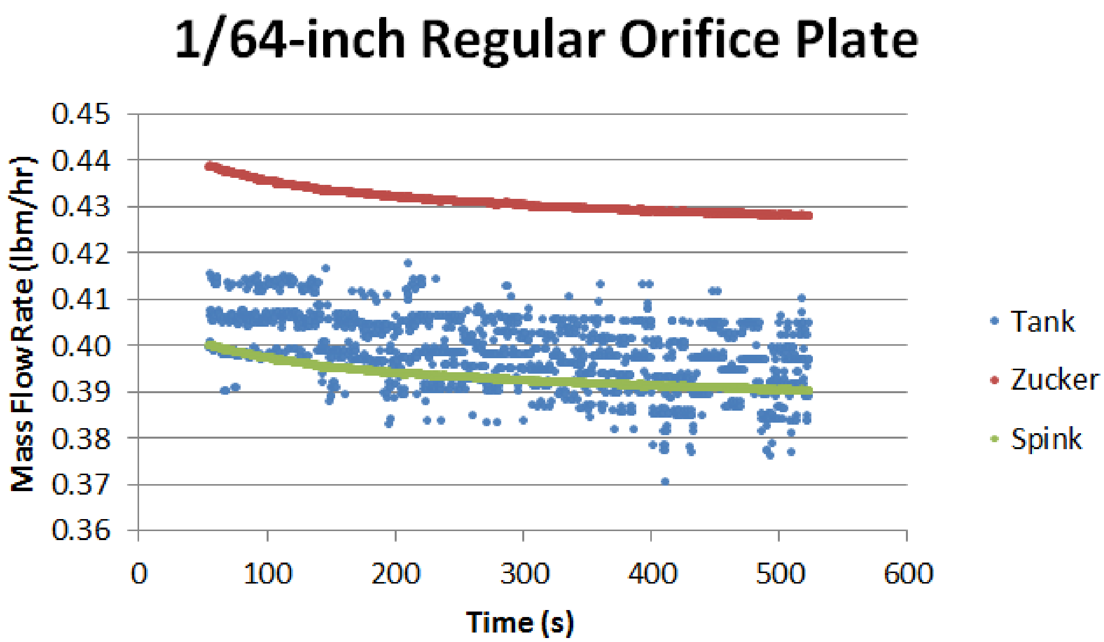

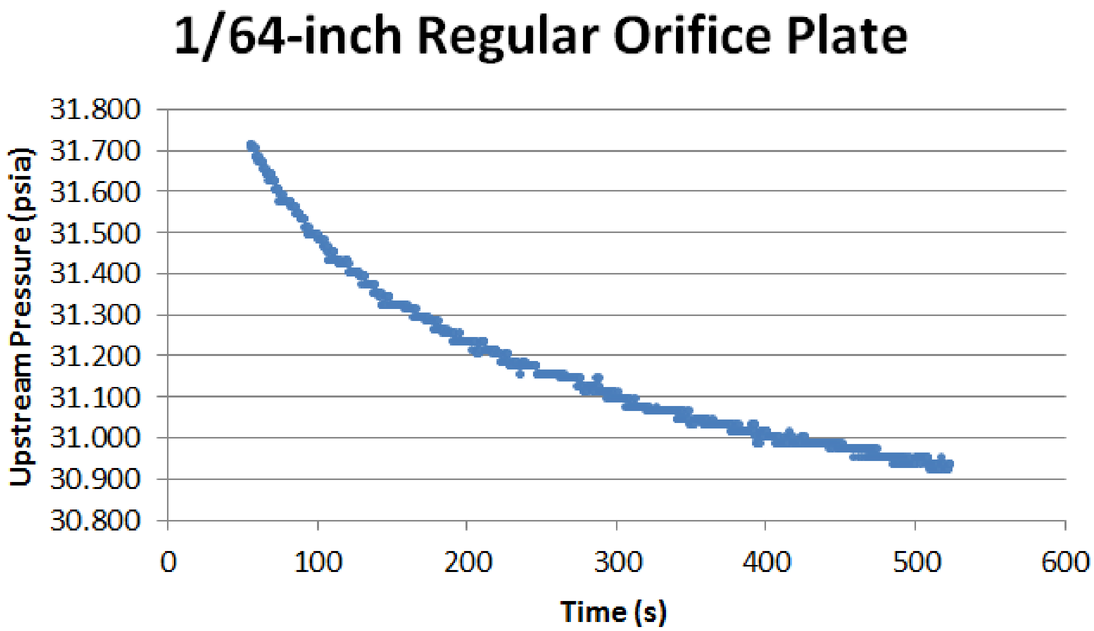

Figure 18, 1/64-inch Regular Orifice Plate Test Graphs

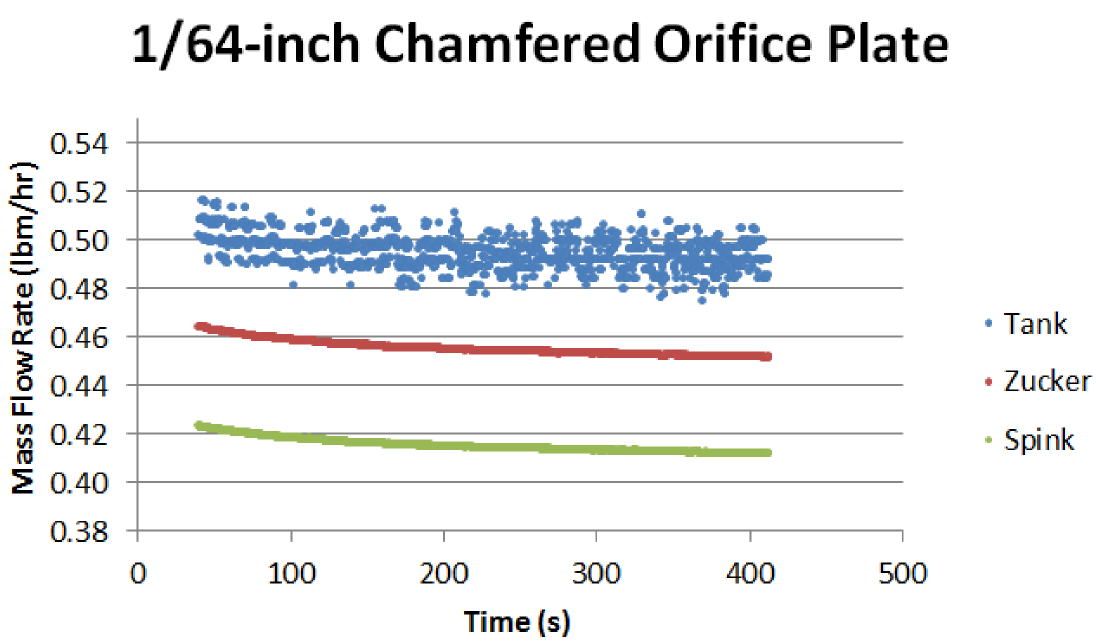

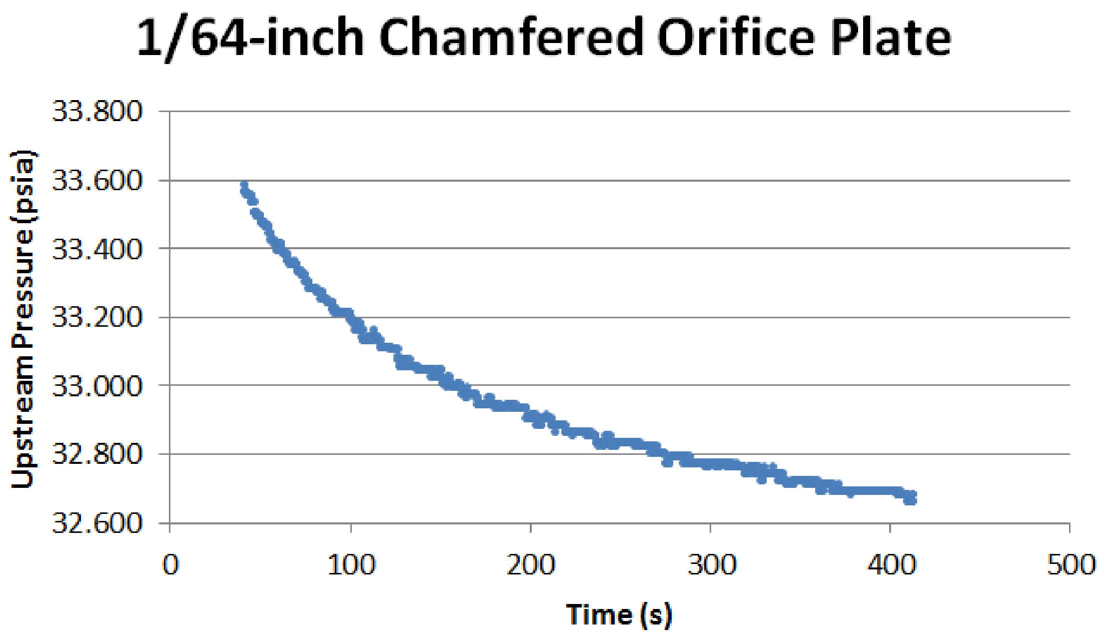

Figure 19, 1/64-inch Chamfered Orifice Plate Test Graphs

It is important to verify that critical flow is occurring during the test. The graphs show that the mass flow rate for each orifice remains constant with a slight decline. When looking at the upstream pressure verses time graph, the upstream pressure decreases with time. This explains why the mass flow rate was decreasing for each test. If the upstream pressure decreases then the mass flow rate will also decrease. If a high quality pressure regulator would have been used, then the upstream pressure would have remained constant, and in turn, caused the mass flow rate to also remain constant.

It is interesting to note that the tank equation curve is very noisy. The literature review mentioned this, "A related disadvantage of the critical flow meter is the acoustical disturbance created in the downstream fluid…The resulting shock waves cause acoustical noise and turbulence, which may affect apparatus performance and downstream measurements in some applications" (Reference 4). For example, the tank temperature data verses time was plotted for the 1/16-inch orifice plate and is shown in Figure 20. This graph shows the level of noise present in the temperature measurements.

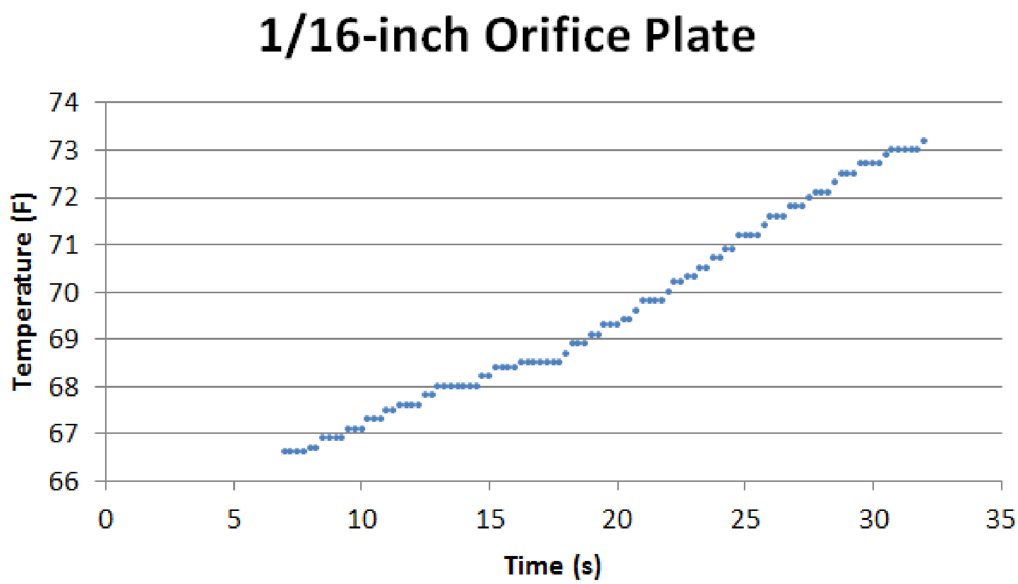

Figure 20, Tank Temperature Graph

It was observed that the 1/16-inch diameter orifice discharged the nitrogen 4 times faster than then the 1/32-inch diameter orifice, and 16 times faster than the 1/64-inch diameter orifices. The flow rates differ by a ratio of the square of the respective diameters. This is why a diameter twice as big produces a mass flow rate four times greater than the diameter twice as small.

Equations 7 and 9 were used to calculate the theoretical mass flow rate, while Equation 16 was used to calculate the actual mass flow rate. Equation 5 was not used, because it was not possible to measure the flow conditions at the throat of the vena contracta with available instrumentation. This is due to the assumption than no losses are present in the form of a discharge coefficient. When calculating the actual conditions from Equation 16, the time step must receive special attention. If the time step is too small, then Equation 16 will produce poor results. This is due to instrumentation noise.

The DAQ recorded conditions every ¼ of a second, so if that were to be used as the calculating time step, then the difference would negligible. For this reason, the 1/16" orifice plate was calculated using a 5 second time step, the 1/32" orifice plate was calculated using a 10 second time step, and the #78 orifice plate was calculated using a 15 second time step.

The calculated average mass flow rates with uncertainties are reported in Table 8.

Table 8, Average Mass Flow Rates with Uncertainties

Orifice Plate	Measure Flow Rate				Theoretical Equations							
	Ideal Gas				Zucker				Spink			
1/16-inch	6.235	+/-	0.2824	lbm/hr	6.669	+/-	0.0984	lbm/hr	6.494	+/-	0.3308	lbm/hr
1/32-inch	1.765	+/-	0.2698	lbm/hr	1.661	+/-	0.0346	lbm/hr	1.500	+/-	0.1593	lbm/hr
1/64-inch Regular	0.399	+/-	0.2733	lbm/hr	0.431	+/-	0.0124	lbm/hr	0.393	+/-	0.0670	lbm/hr
1/64-inch Chamfered	0.495	+/-	0.2706	lbm/hr	0.456	+/-	0.0131	lbm/hr	0.415	+/-	0.0708	lbm/hr

Chapter VIII: Conclusions

Conclusions fall into two distinct areas regarding: (i) the uncertainties in the critical mass flow rate that should be expected by a researcher using critical flow orifices when using standard calculation practices while observing recommended experimental standard practices and (ii) observations regarding the advantages of using critical flow orifices vis-à-vis other critical flow measurement devices such as a critical flow nozzle or venture.

Uncertainties in the Critical Mass Flow Rate Calculated Using Standard Practices

The calculational uncertainty using Zucker's equation was found to be ±1.5% for the 1/16-inch diameter orifice, , ±2.1% for the 1/32-inch diameter orifice, and ±2.9% for both of the 1/64-inch diameter orifices. The calculational uncertainty using Spink's equation was found to be ±5.1% for the 1/16-inch diameter orifice, , ±10.6% for the 1/32-inch diameter orifice, and ±17.0% for both of the 1/64-inch diameter orifices. As previously discussed, the Spink equation is an outdated methodology which is of limited use for the purpose of this research in part because a trend-line approximation was required to perform the mass flow rate calculations for the 1/32-inch and 1/64-inch diameter orifices. Therefore the Zucker equation is recommended and the above calculational accuracies, ranging from ±1.5% for the 1/16-inch diameter orifice to ±2.9% for the 1/64-inch diameter orifice are reasonable and acceptable for many applications.

Virtues of Using Critical Flow Orifices

Compared to other types of flow meters, a critical flow orifice meter is relatively simple to construct and can be constructed very quickly. In addition it is very inexpensive to construct a critical flow orifice. For these reasons, the critical flow orifice meter may be preferred over other meters, even if it may not be as accurate. To minimize the measurement uncertainty the critical flow orifice may be calibrated in situ.

Future Research Possibilities/Questions for Future Inquiry

A possible future study would be to test how the mass flow rate changes as you approach the critical pressure ratio. Also, another similar future study would be to vary the upstream pressure and see if the total percent error would change. This information would be important if a critical flow orifice meter were to be used at differing upstream pressures.

References

1. Busch, Vacuum Pumps and Systems. Flow Through An Orifice: How Orifice Size is Useful in Vacuum Pump Selection. Retrieved from http://www.buschusa.com/fileadmin/Companies/USA/Pictures/Systems/Flow_Through_An_Orifice.pdf

2. Kurita, C.H. (1988). Critical Flow Restricting Orifices. Retrieved from http://lss.fnal.gov/archive/d0-en/fermilab-d0-en-173.pdf

3. Urone, P & Ross, R. (1979). Pressure Change Effects on Hypodermic Needle. Critical Orifice Air Flow Rates. *American Chemical Society, Volume 13, Number 3*. Retrieved from http://pubs.acs.org/doi/abs/10.1021/es60151a016?journalCode=esthag

4. Perry, Jr., J. A. Critical Flow Through Sharp-Edged Orifices, Trans. ASME, 71: 737: 1949

5. Ward, A. & Smith, J. (1979). Critical Flowmetering: The Characteristics of Cylindrical Nozzles with Sharp Upstream Edges. *International Journal of Heat and Fluid Flow, Vol:1, pp. 123-132.*

6. Brain, T. J. S., and Reid, J. Performance of small diameter cylindrical critical flow nozzles, National Engineering Laboratory Report 546, 1975.

7. Deckker, B. E. L., and Chang, Y.F. An investigation of steady compressible flow of air through square edged orifices, Proc. Instn. Mech. Engrs., 1965-66, 180, (Pt. 3J), 312-323

8. Jackson, R. A. The compressible discharge of air through small thick plate orifices, Appl. Scient. Res., Section A, 1963, 13, 241-248

9. Grace, H.P., and Lapple, C. E. Discharge coefficients of small diameter orifices and flow nozzles, Trans. Am. Soc. Mech. Engrs., 1951, 73, 639-647

10. Kastner, L. J., Williams, T.J., and Sowden, R. A. Critical-flow nozzle meter and its application to the measurement of mass flow rate in steady and pulsating streams of gas, J. Mech, Engng. Sci., 1964, 6, (1), 88-98

11. Rohde, J. E., Richards, H. T., and Metger, G. W. Discharge coefficients for thick plate orifices with approach flow perpendicular and inclined to the orifice axis, National Aeronautics and Space Administration NANA TN D-5467, 1969

12. Zimmerman, N & Reist, P. (1984). The Critical Orifice Revisited: A Novel Low Pressure Drop Critical Orifice. *American Industrial Hygiene Association Journal, Vol: 45, pp. 340-344.*

13. Stanton, T. E. On the Flow of Gases at High Speed. Proc. R. Soc. London 111, 306-339, 1926

14. Spink, L.K. (1967). Principles and Practice of Flow Meter Engineering: Ninth Edition. Foxboro, Massachusetts, USA: The Foxboro Company.

15. Zucker, R & Biblarz, O. (2002). Fundamentals of Gas Dynamics: Second Edition. Hoboken, New Jersey: John Wiley & Sons, Inc.

16. Miller, R.W., Flow Measurement Engineering Handbook, McGraw-Hill Co, page 13-4, equation 13.9, 1983

17. Cengel, Y & Boles, M. (2008). Thermodynamics, An Engineering Approach: Sixth Edition. New York, NY: The McGraw-Hill Companies Inc.

18. *Measurement Uncertainty for Fluid Flow in Closed Conduits*. ANSI/ASME MFC-2M-1983. An American National Standard. New York, NY: The American Society of Mechanical Engineers

Appendices

Appendix A: Orifice Area & Downstream Volume Calculation Procedure

Pixel Counting

This is accomplished by scanning an orifice plate at a high resolution. The image can then be magnified until each individual pixel can be detected and counted. A pixel that lies on the orifice region will be a different color from a pixel that lies on the orifice plate material. If a pixel lies on the edge of the orifice and the plate, the color will be in between the color of the orifice and the color of the plate. The shade of the pixel will determine how much of the total pixel area lies over the edge.

Using two separate scanners, two images of a single orifice plate were used to determine how many pixels each orifice contained. The pixels that were located on the edge of the orifice were also counted. Each scanned image has a resolution in terms of dots per inch (dpi). If the resolution is 600 dpi, this means that there are 600 dots per linear inch. Two dots in the horizontal direction and two dots in the vertical direction make up a pixel. A pixel is basically a square made up of equal sides that are the length of a dot. To calculate the area of the orifice based on the number of pixels, use this equation

$$A = \frac{\#\ of\ Pixels}{(dpi)^2}$$

where that area is reported in squared inches. Figure 21 is a zoomed printed image produced from both scanners. It shows the contrast between the hole and orifice plate.

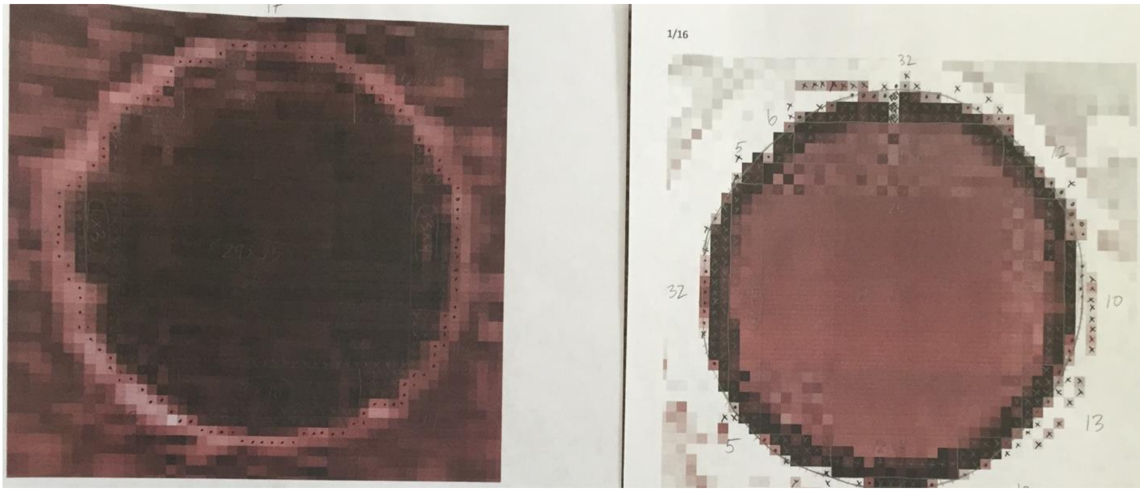

Figure 21, Pixel Counting

The circumference of the orifice is directly related to the number of pixels that occupy the edge of the orifice. By using the circumference of the orifice, the number of dots per inch can be calculated along with the number of pixels that occupy the edge. The calculated number of pixels on the edge is very close to the number of pixels physically counted on the edge of the orifice on the scanned image. It will be assumed that the area of the orifice is calculated based on the diameter of the drill bit that drilled the hole plus or minus the area of the pixels that occupy the edge of the orifice. It was determined that level of uncertainty of the orifice area is as follows: 1/16-inch orifice –> 0.00307+/- 0.000167 in^2, 1/32-inch orifice –> 0.000767+/- 0.0000833 in^2, 1/64-inch orifice –> 0.000201+/- 0.0000416 in^2.

Determining the Volume and Uncertainty Downstream of the Orifice Plate

The volume downstream of the orifice was determined by adding water to the receiver tank, vacuum line, DPT line, and the DPT, and then measuring this water with a 2000 mL graduated cylinder. Water was added to the receiver tank through the vacuum line, and the air was bled from the lid surface by loosening the fittings on the lid. The tank was constantly moved and vibrated to work the air bubbles out of the lid surface. The 2000 mL graduated cylinder that was used, had 20 mL incremental measuring lines. All measurements were made by using the 20 mL lines on the graduated cylinder. Using a +/- 20 mL for each individual measurement with 14 total measurements, equals +/- 280 mL or +/- 0.00988 ft^3 level of uncertainty on the total volume. The total volume was found to be 26.8325 Liters or 0.94758 ft^3.

Another method for determining the volume of the receiver tank was used. The receiver tank was weighed initially dry, and then again after water was added. This method proved to have too high of an uncertainty, because a low precision scale that was used. An uncertainty of 1 lb of water converts to 2 cups of volume. If a more precise scale had been used, this method would have worked.

Appendix B: Calibration Process & Leak Test

Calibration Process

The thermocouples, DPTs, and the DAQ all must calibrated together in order to produce accurate results. The DPTs were calibrated by using a pressure calibrator, as seen in Figure 22. A pressure calibrator is a trusted device that shows the actual pressure reading in comparison to the DPT's reading. This pressure calibrator was connected to each DPT for calibration. The DAQ that was used for this experiment had an upper and lower range setting to automatically convert a voltage measurement to a pressure reading. Both DPTs pressure readings showed deviation from the calibrator readings near the beginning and ending of the of the DPT's range. It was determined to ignore data received from the DAQ at these upper and lower ranges. It was confirmed that the DPTs, within the acceptable ranges, were calibrated and producing pressure readings accurately.

Figure 22, Pressure Calibrator

The thermocouples were calibrated by using a trusted/calibrated thermometer. An ice bath and hot water bath were also used with the calibrated thermometer and thermocouple, to verify that the thermocouples were producing accurate temperature readings. This calibration process confirmed that the thermocouples were calibrated and working properly.

Leak Test

Two types of leak tests were performed to verify that the test apparatus was not leaking from the fittings or connections. The first leak test was accomplished by adding pressurized air (40 psig) to the receiver tank and using a water/soap solution to detect leaks in the form of bubbles. Initially, Teflon tape was used on the threaded connections, but the bubble leak test revealed that the Teflon tape did not prevent leaks. The Teflon tape was then replaced with a pipe thread dope sealant. The leak test was performed again, and found that the pipe dope sealed and prevent leaks from occurring. This test can be seen in Figure 23.

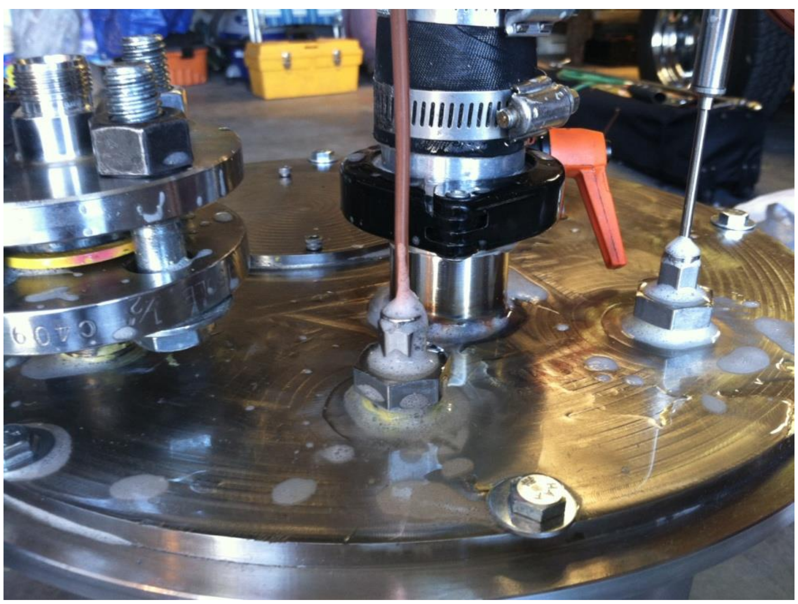

Figure 23, Bubble Leak Test

The next leak test consisted of pulling a vacuum and monitoring the system pressure with respect to time. This leak test was performed in conjunction with the actual testing. The pressure in the system was reduced to 3x10^-3 Torr, and was able to maintain that pressure for15 minutes. This leak test was repeated for each orifice plate to insure that no leaking was occurring between the flange fitting and orifice plate after changing each of the orifice plates.

Appendix C: Calculation Examples

Tank Mass Flow Equation

Tank Equation 1 / 16 "

Test Data # 70 & 90

In[71]:=
```
R = 0.3830; (*[psia*ft^3/lbm*R] N2 Gas Constant*)
V = 0.947581; (*[ft^3] Tank Volume*)
Pg1 = -7.135; (*[psig] Tank Pressure 1*)
P1 = Pg1 + 12.50; (*[psia] Tank Pressure 1*)
Pg2 = -5.251; (*[psig] Tank Pressure 2*)
P2 = Pg2 + 12.50; (*[psia] Tank Pressure 2*)
TF1 = 68.5; (*[F] Tank Temperature 1*)
T1 = TF1 + 459.67; (*[R] Tank Temperature 1*)
TF2 = 70.2; (*[F] Tank Temperature 2*)
T2 = TF2 + 459.67; (*[R] Tank Temperature 2*)
t1 = 17.25; (*[sec] Time 1*)
t2 = 22.25; (*[sec] Time 2*)
```

$$mdot = \frac{\frac{V}{R} * \left(\frac{P2}{T2} - \frac{P1}{T1}\right)}{t2 - t1};$$ (*[lbm/sec] Mass Flow Rate Equation*)

```
mdotHR = mdot * 3600 (*[lbm/hr] Mass Flow Rate Equation*)
```

Out[74]= 6.27571

Tank Mass Flow Uncertainty Equation

Tank Uncertainty Equation 1/16”

Test Data # 70 & 90

In[1]:= $\text{mdot} = \dfrac{\frac{V}{R} * \left(\frac{P2}{T2} - \frac{P1}{T1}\right)}{t2 - t1}$ (*Mass Equation*)

Out[1]= $\dfrac{\left(-\frac{P1}{T1} + \frac{P2}{T2}\right) V}{R\,(-t1 + t2)}$

In[2]:= $(D[\text{mdot}, V] * SV)^2$

$(D[\text{mdot}, P1] * SP)^2$

$(D[\text{mdot}, P2] * SP)^2$

$(D[\text{mdot}, T1] * ST)^2$

$(D[\text{mdot}, T2] * ST)^2$

Out[2]= $\dfrac{SV^2 \left(-\frac{P1}{T1} + \frac{P2}{T2}\right)^2}{R^2\,(-t1 + t2)^2}$

Out[3]= $\dfrac{SP^2\,V^2}{R^2\,T1^2\,(-t1 + t2)^2}$

Out[4]= $\dfrac{SP^2\,V^2}{R^2\,(-t1 + t2)^2\,T2^2}$

Out[5]= $\dfrac{P1^2\,ST^2\,V^2}{R^2\,T1^4\,(-t1 + t2)^2}$

Out[6]= $\dfrac{P2^2\,ST^2\,V^2}{R^2\,(-t1 + t2)^2\,T2^4}$

Out[12]= $\dfrac{P2^2\,ST^2\,V^2}{R^2\,(-t1 + t2)^2\,T2^4}$

```
In[20]:= R = 0.3830; (*[psia*ft^3/lbm*R] N2 Gas Constant*)
V = 0.947581; (*[ft^3] Tank Volume*)
T1 = 528.17; (*[R] Tank Temperature*)
T2 = 529.87; (*[R] Tank Temperature*)
P1 = 5.365; (*[psia] Tank Pressure 1*)
P2 = 7.249; (*[psia] Tank Pressure 2*)
t1 = 17.25; (*[s] time 1*)
t2 = 22.25; (*[s] time 2*)
SV = .00988; (*[ft^3] Tank Volume Uncertainty*)
ST = 2.06; (*[F] Tank Temperature Uncertainty*)
SP = .02778; (*[psi] Tank Pressure Uncertainty*)
```

$$\text{mdot} = \left(\frac{SV^2\left(-\frac{P1}{T1}+\frac{P2}{T2}\right)^2}{R^2(-t1+t2)^2} + \frac{SP^2\,V^2}{R^2\,T1^2\,(-t1+t2)^2} + \frac{SP^2\,V^2}{R^2\,(-t1+t2)^2\,T2^2} + \frac{P1^2\,ST^2\,V^2}{R^2\,T1^4\,(-t1+t2)^2} + \frac{P2^2\,ST^2\,V^2}{R^2\,(-t1+t2)^2\,T2^4}\right)^{\frac{1}{2}}$$
; (*[lbm/s] Mass Flow Uncertainty*)

```
mdotHR = mdot * 3600 (*[lbm/hr] Mass Flow Uncertainty*)
Out[23]= 0.189049
```

Zucker Mass Flow Equation

Zucker's Equation 1/16"

Test Data # 70

In[1]:=

```
Cd = 0.839; (*Discharge Coefficient*)
γ = 1.4; (*Specifice Heat Ratio of N2*)
di = 1 / 16; (*[in] Orifice Diameter*)
d = di / 39.370; (*[m] Orifice Diameter*)
R = 0.2968; (*[R*kJ/kg*K] N2 Gas Constant*)
Pg = 18.74; (*[psig] Upstream Stagnation Pressure*)
Pa = Pg + 12.50; (*[psia] Upstream Stagnation Pressure*)
P = Pa * 6.894757; (*[kPa] Upstream Stagnation Pressure*)
TF = 67.5; (*[F] Upstream Stagnation Temperature*)
TR = TF + 459.67; (*[R] Upstream Stagnation Temperature*)
T = TR / 1.8; (*[K] Upstream Stagnation Temperature*)
```

$A = \frac{\pi}{4} * d^2;$ (*[m^2] Orifice Area*)

$\rho = \frac{P * 1000}{R * T};$ (*[kg/m^3]Upstream Stagnation Pressure*)

$mdot = Cd * A * \left(\gamma * \rho * P * \left(\frac{2}{\gamma + 1}\right)^{\frac{\gamma+1}{\gamma-1}}\right)^{\frac{1}{2}};$ (*[kg/s]Mass Flow Rate*)

```
mdotHR = mdot * 3600 * 2.2046226 (*[lbm/hr]Mass Flow Rate*)
```

Out[7]= 6.59321

Zucker Mass Flow Uncertainty Equation

Zucker ' s Uncertainty Equation 1 / 16 " Test Data #70

```
Cd = 0.839; (*Discharge Coefficient*)
γ = 1.4; (*Specific Heat Ratio of N2*)
```

$A = \frac{\pi}{4} * d^2;$ (*Orifice Area*)

$\rho = \frac{P}{R * T};$ (*Upstream Stagnation Density*)

$\text{mdot} = Cd * A * \left(\gamma * \rho * P * \left(\frac{2}{\gamma + 1}\right)^{\frac{\gamma+1}{\gamma-1}}\right)^{\frac{1}{2}};$ (*Mass Flow Rate Equation*)

$(D[\text{mdot}, d] * Sd)^2$ (*Partial Derivative*)

$(D[\text{mdot}, P] * SP)^2$ (*Partial Derivative*)

$(D[\text{mdot}, T] * ST)^2$ (*Partial Derivative*)

$$\frac{0.814337\, d^2\, P^2\, Sd^2}{R\, T}$$

$$\frac{0.203584\, d^4\, SP^2}{R\, T}$$

$$\frac{0.0508961\, d^4\, P^2\, ST^2}{R\, T^3}$$

```
di = 1 / 16; (*[in] Orifice Diameter*)
d = di / 39.370; (*[m] Orifice Diameter*)
R = 0.2968; (*[R*kJ/kg*K] N2 Gas Constant*)
Pg = 18.74; (*[psig] Upstream Stagnation Pressure*)
Pa = Pg + 12.50; (*[psia] Upstream Stagnation Pressure*)
P = Pa * 6.894757; (*[kPa] Upstream Stagnation Pressure*)
TF = 67.5; (*[F] Upstream Stagnation Temperature*)
TR = TF + 459.67; (*[R] Upstream Stagnation Temperature*)
T = TR / 1.8; (*[K] Upstream Stagnation Temperature*)
Sdi = 0.01458; (*[in] Diameter Uncertainty*)
Sd = Sdi / 39.370; (*[m] Diameter Uncertainty*)
STF = 2.06; (*[K] Upstream Temperature Uncertainty*)
ST = STF / 1.8; (*[K] Upstream Temperature Uncertainty*)
Sp = 0.0375; (*[psi] Upstream Pressure Uncertainty*)
SP = Sp * 6.894757; (*[kPa] Upstream Pressure Uncertainty*)
```

$$\text{Smdot} = \left(\frac{0.814337\, d^2\, P^2\, Sd^2}{R\, T} + \frac{0.203584\, d^4\, SP^2}{R\, T} + \frac{0.0508961\, d^4\, P^2\, ST^2}{R\, T^3}\right)^{\frac{1}{2}};$$

```
(*Total Mass Flow Rate Uncertainty*)
SmdotHR = Smdot * 3600 * 2.2046226 (*[lbm/hr]Mass Flow Rate*)
0.0972769
```

Spink Mass Flow Equation

Spink's Equation 1 / 16 "

Test Data # 70

```
In[29]:= YtSp = 0.04; (*value determined from Fig. B-2525 of Spink*)
Fa = 1; (*Temperature Expansion Factor*)
De = 0.43; (*[in] Entrance Diameter*)
R = 0.3830; (*[psia*ft^3/lbm*R] N2 Gas Constant*)
Pg = 18.74; (*[psig] Upstream Stagnation Pressure*)
P = Pg + 12.50;  (*[psia] Upstream Stagnation Pressure*)
TF = 67.5;  (*[F] Upstream Stagnation Temperature*)
T = TF + 459.67;  (*[R] Upstream Stagnation Temperature*)
γ = P/(T * R);  (*[lb/ft^3]Specific Weight*)
mdot = 359 * YtSp * De^2 * Fa * (γ)^.5 * (P)^.5 (* [lbm/hr] mass flow rate*)

Out[34]= 5.83751
```

Spink Mass Flow Uncertainty Equation

Spink's Uncertainty Equation 1/16" Test Data #70

```
In[1]:= R = 0.383; (*N2 Gas Constantt*)
        γ = P/(T*R); (*Density*)
        uD = 0.43;
        YtSp = 1.9726*(d/uD)^2.0083;

        mdot = 359*YtSp*uD^2*1*(γ)^.5*(P)^.5;(*Mass Flow Rate Equation*)
        (D[mdot, P]*SP)^2(*Partial Derivative times Pt uncertainty*)
        (D[mdot, T]*ST)^2(*Partial Derivative times T uncertainty*)
        (D[mdot, d]*Sd)^2
        (*Partial Derivative times d uncertainty*)
```

Out[6]= $SP^2\left(\frac{576.164\ d^{2.0083}\left(\frac{P}{T}\right)^{0.5}}{P^{0.5}}+\frac{576.164\ d^{2.0083}\ P^{0.5}}{\left(\frac{P}{T}\right)^{0.5}\ T}\right)^2$

Out[7]= $\frac{331965.\ d^{4.0166}\ P^{3.}\ ST^2}{\left(\frac{P}{T}\right)^{1.}\ T^4}$

Out[8]= $5.35562\times10^6\ d^{2.0166}\ P^{1.}\ Sd^2\left(\frac{P}{T}\right)^{1.}$

```
d = 0.0625;
Pg = 18.74; (*[psig] Upstream Stagnation Pressure*)
P = Pg + 12.50; (*[psia] Upstream Stagnation Pressure*)
TF = 67.5; (*[F] Upstream Stagnation Temperature*)
T = TF + 459.67; (*[R] Upstream Stagnation Temperature*)
ST = 2.06; (*[K] Upstream Temperature Uncertainty*)
SP = .0375   (*[psi] Upstream Pressure Uncertainty*)
Sd = .001699;
Smdot =
```

$$\left(SP^2\left(\frac{576.164\ d^{2.0083}\left(\frac{P}{T}\right)^{0.5}}{P^{0.5}}+\frac{576.164\ d^{2.0083}\ P^{0.5}}{\left(\frac{P}{T}\right)^{0.5}\ T}\right)^2+\frac{331\,965\ d^{4.0166}\ P^{3.}\ ST^2}{\left(\frac{P}{T}\right)\ T^4}+5.35562*^6\ d^{2.0166}\ P\ Sd^2\left(\frac{P}{T}\right)\right)^{\frac{1}{2}}$$ (*[lbm/hr] Mass Flow Uncertainty*)

Out[9]= 0.332076

Appendix D: Test Data Report

1/16-inch Orifice Plate

Vendor	GRAPHTEC Corp.						
Model	GL820						
Version	Ver1.03						
Sampling interval	250ms						
Total data points	151						
Start time	11/17/2014	12:47:56					
End time	11/17/2014	12:48:34					
Trigger time	11/17/2014	12:47:56					
AMP settings							
CH	Signal name	Input	Range	Filter	Span		
CH1	P TANK	DC	50V	Off	-64.106	69.503	[psi]
CH2	P UPSTREAM	DC	50V	Off	149.5	-161.75	[psi]
CH3	T TANK	TEMP	TC_K	Off	3000	-200	[degF]
CH4	T UPSTREAM	TEMP	TC_K	Off	3000	-200	[degF]
Logic/Pulse	Off						
Data							

Number	Date&Time	ms	CH1	CH2	CH3	CH4
NO.	Time	ms	psi	psi	degF	degF
20	11/17/2014 12:48	750	-11.631	19.51	66	67.8
21	11/17/2014 12:48	0	-11.617	19.49	66	67.8
22	11/17/2014 12:48	250	-11.577	19.49	66	68
23	11/17/2014 12:48	500	-11.524	19.44	66	68
24	11/17/2014 12:48	750	-11.45	19.41	66.2	67.8
25	11/17/2014 12:48	0	-11.363	19.4	66.2	67.8
26	11/17/2014 12:48	250	-11.263	19.37	66.2	67.8
27	11/17/2014 12:48	500	-11.163	19.34	66.4	67.8
28	11/17/2014 12:48	750	-11.076	19.32	66.6	67.8
29	11/17/2014 12:48	0	-10.976	19.29	66.6	67.8
30	11/17/2014 12:48	250	-10.882	19.27	66.6	67.8
31	11/17/2014 12:48	500	-10.789	19.24	66.6	67.8
32	11/17/2014 12:48	750	-10.689	19.23	66.6	67.6
33	11/17/2014 12:48	0	-10.595	19.2	66.7	67.8
34	11/17/2014 12:48	250	-10.495	19.18	66.7	67.8
35	11/17/2014 12:48	500	-10.408	19.15	66.9	67.6
36	11/17/2014 12:48	750	-10.315	19.15	66.9	67.6
37	11/17/2014 12:48	0	-10.214	19.12	66.9	67.6
38	11/17/2014 12:48	250	-10.121	19.1	66.9	67.6
39	11/17/2014 12:48	500	-10.027	19.09	67.1	67.6
40	11/17/2014 12:48	750	-9.934	19.06	67.1	67.6
41	11/17/2014 12:48	0	-9.84	19.06	67.1	67.6
42	11/17/2014 12:48	250	-9.753	19.04	67.3	67.6

43	11/17/2014 12:48	500	-9.653	19.02	67.3	67.6
44	11/17/2014 12:48	750	-9.566	19.01	67.3	67.6
45	11/17/2014 12:48	0	-9.473	18.99	67.5	67.8
46	11/17/2014 12:48	250	-9.379	18.98	67.5	67.6
47	11/17/2014 12:48	500	-9.286	18.98	67.6	67.8
48	11/17/2014 12:48	750	-9.192	18.96	67.6	67.6
49	11/17/2014 12:48	0	-9.099	18.95	67.6	67.6
50	11/17/2014 12:48	250	-9.012	18.93	67.6	67.6
51	11/17/2014 12:48	500	-8.918	18.92	67.8	67.6
52	11/17/2014 12:48	750	-8.825	18.9	67.8	67.6
53	11/17/2014 12:48	0	-8.731	18.88	68	67.6
54	11/17/2014 12:48	250	-8.631	18.87	68	67.6
55	11/17/2014 12:48	500	-8.538	18.87	68	67.6
56	11/17/2014 12:48	750	-8.444	18.85	68	67.6
57	11/17/2014 12:48	0	-8.351	18.85	68	67.6
58	11/17/2014 12:48	250	-8.257	18.84	68	67.6
59	11/17/2014 12:48	500	-8.157	18.82	68	67.6
60	11/17/2014 12:48	750	-8.07	18.81	68.2	67.5
61	11/17/2014 12:48	0	-7.976	18.81	68.2	67.5
62	11/17/2014 12:48	250	-7.883	18.81	68.4	67.5
63	11/17/2014 12:48	500	-7.783	18.79	68.4	67.5
64	11/17/2014 12:48	750	-7.689	18.78	68.4	67.5
65	11/17/2014 12:48	0	-7.602	18.79	68.4	67.5
66	11/17/2014 12:48	250	-7.509	18.78	68.5	67.6
67	11/17/2014 12:48	500	-7.415	18.78	68.5	67.5
68	11/17/2014 12:48	750	-7.322	18.76	68.5	67.5
69	11/17/2014 12:48	0	-7.228	18.74	68.5	67.5
70	11/17/2014 12:48	250	-7.135	18.74	68.5	67.5
71	11/17/2014 12:48	500	-7.041	18.73	68.5	67.5
72	11/17/2014 12:48	750	-6.941	18.73	68.5	67.5
73	11/17/2014 12:48	0	-6.847	18.71	68.7	67.5
74	11/17/2014 12:48	250	-6.754	18.71	68.9	67.5
75	11/17/2014 12:48	500	-6.66	18.71	68.9	67.5
76	11/17/2014 12:48	750	-6.56	18.68	68.9	67.5
77	11/17/2014 12:48	0	-6.467	18.68	69.1	67.5
78	11/17/2014 12:48	250	-6.373	18.67	69.1	67.5
79	11/17/2014 12:48	500	-6.28	18.67	69.3	67.5
80	11/17/2014 12:48	750	-6.186	18.65	69.3	67.5
81	11/17/2014 12:48	0	-6.093	18.65	69.3	67.5
82	11/17/2014 12:48	250	-6.006	18.65	69.4	67.5
83	11/17/2014 12:48	500	-5.906	18.63	69.4	67.5
84	11/17/2014 12:48	750	-5.819	18.63	69.6	67.5
85	11/17/2014 12:48	0	-5.725	18.63	69.8	67.5

86	11/17/2014 12:48	250	-5.625	18.62	69.8	67.5
87	11/17/2014 12:48	500	-5.538	18.62	69.8	67.5
88	11/17/2014 12:48	750	-5.438	18.6	69.8	67.5
89	11/17/2014 12:48	0	-5.351	18.6	70	67.5
90	11/17/2014 12:48	250	-5.251	18.6	70.2	67.5
91	11/17/2014 12:48	500	-5.164	18.59	70.2	67.5
92	11/17/2014 12:48	750	-5.064	18.59	70.3	67.5
93	11/17/2014 12:48	0	-4.977	18.59	70.3	67.5
94	11/17/2014 12:48	250	-4.877	18.57	70.5	67.5
95	11/17/2014 12:48	500	-4.783	18.57	70.5	67.5
96	11/17/2014 12:48	750	-4.69	18.56	70.7	67.5
97	11/17/2014 12:48	0	-4.596	18.56	70.7	67.5
98	11/17/2014 12:48	250	-4.509	18.57	70.9	67.5
99	11/17/2014 12:48	500	-4.409	18.57	70.9	67.5
100	11/17/2014 12:48	750	-4.316	18.56	71.2	67.6
101	11/17/2014 12:48	0	-4.222	18.56	71.2	67.6
102	11/17/2014 12:48	250	-4.129	18.54	71.2	67.5
103	11/17/2014 12:48	500	-4.035	18.56	71.2	67.5
104	11/17/2014 12:48	750	-3.941	18.54	71.4	67.5
105	11/17/2014 12:48	0	-3.848	18.54	71.6	67.5
106	11/17/2014 12:48	250	-3.748	18.54	71.6	67.5
107	11/17/2014 12:48	500	-3.661	18.54	71.6	67.5
108	11/17/2014 12:48	750	-3.561	18.53	71.8	67.5
109	11/17/2014 12:48	0	-3.46	18.51	71.8	67.5
110	11/17/2014 12:48	250	-3.374	18.51	71.8	67.5
111	11/17/2014 12:48	500	-3.267	18.51	72	67.5
112	11/17/2014 12:48	750	-3.18	18.51	72.1	67.5
113	11/17/2014 12:48	0	-3.08	18.49	72.1	67.5
114	11/17/2014 12:48	250	-2.986	18.49	72.1	67.5
115	11/17/2014 12:48	500	-2.899	18.48	72.3	67.5
116	11/17/2014 12:48	750	-2.799	18.49	72.5	67.5
117	11/17/2014 12:48	0	-2.706	18.48	72.5	67.5
118	11/17/2014 12:48	250	-2.605	18.48	72.5	67.5
119	11/17/2014 12:48	500	-2.519	18.48	72.7	67.5
120	11/17/2014 12:48	750	-2.425	18.48	72.7	67.5
121	11/17/2014 12:48	0	-2.331	18.48	72.7	67.5
122	11/17/2014 12:48	250	-2.238	18.48	72.7	67.3
123	11/17/2014 12:48	500	-2.151	18.46	72.9	67.3
124	11/17/2014 12:48	750	-2.058	18.46	73	67.3
125	11/17/2014 12:48	0	-1.957	18.48	73	67.3
126	11/17/2014 12:48	250	-1.864	18.46	73	67.3
127	11/17/2014 12:48	500	-1.77	18.46	73	67.3
128	11/17/2014 12:48	750	-1.677	18.46	73	67.3

129	11/17/2014 12:48	0	-1.583	18.46	73.2	67.3
130	11/17/2014 12:48	250	-1.496	18.46	73.4	67.3
131	11/17/2014 12:48	500	-1.396	18.45	73.4	67.3
132	11/17/2014 12:48	750	-1.303	18.45	73.6	67.5
133	11/17/2014 12:48	0	-1.209	18.45	73.6	67.3
134	11/17/2014 12:48	250	-1.116	18.43	73.6	67.5
135	11/17/2014 12:48	500	-1.022	18.43	73.8	67.3
136	11/17/2014 12:48	750	-0.929	18.43	73.8	67.3
137	11/17/2014 12:48	0	-0.842	18.43	73.8	67.3
138	11/17/2014 12:48	250	-0.742	18.43	73.9	67.3
139	11/17/2014 12:48	500	-0.655	18.42	73.9	67.3
140	11/17/2014 12:48	750	-0.554	18.42	74.1	67.3
141	11/17/2014 12:48	0	-0.468	18.42	74.1	67.3
142	11/17/2014 12:48	250	-0.374	18.42	74.3	67.5
143	11/17/2014 12:48	500	-0.287	18.4	74.1	67.3
144	11/17/2014 12:48	750	-0.187	18.42	74.5	67.5
145	11/17/2014 12:48	0	-0.1	18.4	74.5	67.5
146	11/17/2014 12:48	250	0	18.4	74.5	67.5
147	11/17/2014 12:48	500	0.087	18.4	74.5	67.5
148	11/17/2014 12:48	750	0.18	18.4	74.5	67.5
149	11/17/2014 12:48	0	0.267	18.39	74.7	67.5
150	11/17/2014 12:48	250	0.367	18.4	74.7	67.5
151	11/17/2014 12:48	500	0.454	18.4	74.7	67.5

1/32-inch Orifice Plate

Vendor	GRAPHTEC Corp.						
Model	GL820						
Version	Ver1.03						
Sampling interval	250ms						
Total data points	490						
Start time	11/17/2014	12:27:48					
End time	11/17/2014	12:29:51					
Trigger time	11/17/2014	12:27:48					
AMP settings							
CH	Signal name	Input	Range	Filter	Span		
CH1	P TANK	DC	50V	Off	-64.106	69.503	[psi]
CH2	P UPSTREAM	DC	50V	Off	149.5	-161.75	[psi]
CH3	T TANK	TEMP	TC_K	Off	3000	-200	[degF]
CH4	T UPSTREAM	TEMP	TC_K	Off	3000	-200	[degF]
Logic/Pulse	Off						
Data							
Number	Date&Time	ms	CH1	CH2	CH3	CH4	
NO.	Time	ms	psi	psi	degF	degF	
20	11/17/14 12:27	750	-11.657	19.58	66	67.5	
22	11/17/14 12:27	250	-11.657	19.52	66	67.5	
24	11/17/14 12:27	750	-11.657	19.49	66.2	67.5	
26	11/17/14 12:27	250	-11.657	19.44	66.2	67.5	
28	11/17/14 12:27	750	-11.657	19.41	66.2	67.5	
30	11/17/14 12:27	250	-11.651	19.4	66.2	67.5	
32	11/17/14 12:27	750	-11.644	19.35	66.6	67.5	
34	11/17/14 12:27	250	-11.637	19.32	66.6	67.5	
36	11/17/14 12:27	750	-11.631	19.3	66.6	67.5	
38	11/17/14 12:27	250	-11.624	19.27	66.6	67.5	
40	11/17/14 12:27	750	-11.604	19.24	66.9	67.5	
42	11/17/14 12:27	250	-11.597	19.23	66.9	67.5	
44	11/17/14 12:27	750	-11.571	19.21	67.1	67.5	
46	11/17/14 12:27	250	-11.544	19.18	67.1	67.5	
48	11/17/14 12:27	750	-11.51	19.15	67.1	67.5	
50	11/17/14 12:28	250	-11.464	19.15	67.3	67.5	
52	11/17/14 12:28	750	-11.417	19.13	67.5	67.5	

54	11/17/14 12:28	250	-11.363	19.12	67.5	67.5
56	11/17/14 12:28	750	-11.31	19.09	67.6	67.5
58	11/17/14 12:28	250	-11.257	19.07	67.6	67.5
60	11/17/14 12:28	750	-11.203	19.06	67.8	67.5
62	11/17/14 12:28	250	-11.15	19.06	67.8	67.5
64	11/17/14 12:28	750	-11.09	19.04	68	67.5
66	11/17/14 12:28	250	-11.049	19.04	68	67.3
68	11/17/14 12:28	750	-10.989	19.02	68.2	67.3
70	11/17/14 12:28	250	-10.936	19.01	68.4	67.3
72	11/17/14 12:28	750	-10.876	18.99	68.4	67.3
74	11/17/14 12:28	250	-10.822	18.99	68.4	67.3
76	11/17/14 12:28	750	-10.762	18.98	68.5	67.3
78	11/17/14 12:28	250	-10.709	18.96	68.5	67.3
80	11/17/14 12:28	750	-10.655	18.95	68.5	67.3
82	11/17/14 12:28	250	-10.609	18.95	68.7	67.3
84	11/17/14 12:28	750	-10.542	18.93	68.9	67.3
86	11/17/14 12:28	250	-10.495	18.92	68.9	67.1
88	11/17/14 12:28	750	-10.435	18.9	69.1	67.3
90	11/17/14 12:28	250	-10.388	18.9	69.1	67.3
92	11/17/14 12:28	750	-10.335	18.88	69.1	67.3
94	11/17/14 12:28	250	-10.275	18.88	69.3	67.3
96	11/17/14 12:28	750	-10.221	18.88	69.3	67.1
98	11/17/14 12:28	250	-10.168	18.87	69.3	67.1
100	11/17/14 12:28	750	-10.114	18.85	69.6	67.5
102	11/17/14 12:28	250	-10.054	18.85	69.4	67.1
104	11/17/14 12:28	750	-10.007	18.85	69.8	67.3
106	11/17/14 12:28	250	-9.954	18.84	69.6	67.1
108	11/17/14 12:28	750	-9.9	18.82	69.8	67.1
110	11/17/14 12:28	250	-9.847	18.84	69.8	67.3
112	11/17/14 12:28	750	-9.8	18.82	69.8	67.3
114	11/17/14 12:28	250	-9.74	18.82	70	67.3
116	11/17/14 12:28	750	-9.687	18.82	70.2	67.3
118	11/17/14 12:28	250	-9.633	18.81	70.2	67.3
120	11/17/14 12:28	750	-9.58	18.81	70.2	67.3
122	11/17/14 12:28	250	-9.526	18.81	70.3	67.3
124	11/17/14 12:28	750	-9.473	18.79	70.3	67.3
126	11/17/14 12:28	250	-9.419	18.79	70.3	67.3
128	11/17/14 12:28	750	-9.366	18.79	70.5	67.3
130	11/17/14 12:28	250	-9.313	18.78	70.5	67.3
132	11/17/14 12:28	750	-9.246	18.76	70.5	67.3
134	11/17/14 12:28	250	-9.199	18.76	70.7	67.5
136	11/17/14 12:28	750	-9.139	18.74	70.7	67.3
138	11/17/14 12:28	250	-9.092	18.74	70.9	67.5

140	11/17/14 12:28	750	-9.032	18.73	70.9	67.3
142	11/17/14 12:28	250	-8.985	18.73	70.9	67.3
144	11/17/14 12:28	750	-8.925	18.71	70.9	67.3
146	11/17/14 12:28	250	-8.878	18.71	70.9	67.3
148	11/17/14 12:28	750	-8.818	18.71	71.1	67.3
150	11/17/14 12:28	250	-8.771	18.71	71.2	67.3
152	11/17/14 12:28	750	-8.711	18.7	71.2	67.3
154	11/17/14 12:28	250	-8.665	18.71	71.2	67.3
156	11/17/14 12:28	750	-8.611	18.71	71.2	67.3
158	11/17/14 12:28	250	-8.558	18.71	71.2	67.3
160	11/17/14 12:28	750	-8.504	18.7	71.2	67.3
162	11/17/14 12:28	250	-8.451	18.7	71.4	67.3
164	11/17/14 12:28	750	-8.391	18.68	71.4	67.3
166	11/17/14 12:28	250	-8.331	18.67	71.6	67.3
168	11/17/14 12:28	750	-8.284	18.67	71.6	67.3
170	11/17/14 12:28	250	-8.23	18.67	71.6	67.3
172	11/17/14 12:28	750	-8.177	18.65	71.8	67.3
174	11/17/14 12:28	250	-8.123	18.65	71.8	67.3
176	11/17/14 12:28	750	-8.077	18.67	71.8	67.1
178	11/17/14 12:28	250	-8.023	18.65	71.8	67.3
180	11/17/14 12:28	750	-7.963	18.65	72	67.3
182	11/17/14 12:28	250	-7.916	18.65	72	67.3
184	11/17/14 12:28	750	-7.863	18.65	72.1	67.3
186	11/17/14 12:28	250	-7.803	18.63	72.1	67.3
188	11/17/14 12:28	750	-7.749	18.63	72.1	67.3
190	11/17/14 12:28	250	-7.696	18.63	72.1	67.3
192	11/17/14 12:28	750	-7.642	18.63	72.1	67.1
194	11/17/14 12:28	250	-7.596	18.63	72.3	67.3
196	11/17/14 12:28	750	-7.536	18.63	72.3	67.1
198	11/17/14 12:28	250	-7.489	18.63	72.3	67.1
200	11/17/14 12:28	750	-7.429	18.62	72.5	67.3
202	11/17/14 12:28	250	-7.375	18.62	72.5	67.3
204	11/17/14 12:28	750	-7.322	18.62	72.5	67.3
206	11/17/14 12:28	250	-7.268	18.62	72.7	67.3
208	11/17/14 12:28	750	-7.215	18.6	72.7	67.3
210	11/17/14 12:28	250	-7.161	18.6	72.5	67.1
212	11/17/14 12:28	750	-7.115	18.6	72.7	67.1
214	11/17/14 12:28	250	-7.055	18.6	72.7	67.3
216	11/17/14 12:28	750	-7.008	18.6	72.7	67.1
218	11/17/14 12:28	250	-6.954	18.59	72.7	67.1
220	11/17/14 12:28	750	-6.908	18.6	72.9	67.1
222	11/17/14 12:28	250	-6.854	18.6	72.9	67.1
224	11/17/14 12:28	750	-6.794	18.6	72.9	67.1

226	11/17/14 12:28	250	-6.747	18.6	73	67.1
228	11/17/14 12:28	750	-6.694	18.6	73	67.1
230	11/17/14 12:28	250	-6.634	18.57	73	67.1
232	11/17/14 12:28	750	-6.58	18.57	73	67.1
234	11/17/14 12:28	250	-6.527	18.57	73	67.1
236	11/17/14 12:28	750	-6.473	18.57	73	67.1
238	11/17/14 12:28	250	-6.42	18.56	73	67.1
240	11/17/14 12:28	750	-6.366	18.56	73	67.1
242	11/17/14 12:28	250	-6.313	18.56	73	67.1
244	11/17/14 12:28	750	-6.26	18.56	73.4	67.3
246	11/17/14 12:28	250	-6.206	18.56	73.4	67.3
248	11/17/14 12:28	750	-6.153	18.56	73.4	67.3
250	11/17/14 12:28	250	-6.099	18.54	73.4	67.3
252	11/17/14 12:28	750	-6.052	18.54	73.6	67.3
254	11/17/14 12:28	250	-5.992	18.54	73.4	67.1
256	11/17/14 12:28	750	-5.946	18.54	73.6	67.3
258	11/17/14 12:28	250	-5.892	18.54	73.6	67.3
260	11/17/14 12:28	750	-5.832	18.54	73.6	67.1
262	11/17/14 12:28	250	-5.785	18.54	73.6	67.3
264	11/17/14 12:28	750	-5.732	18.54	73.8	67.3
266	11/17/14 12:28	250	-5.685	18.54	73.9	67.5
268	11/17/14 12:28	750	-5.632	18.54	73.9	67.5
270	11/17/14 12:28	250	-5.578	18.54	73.9	67.5
272	11/17/14 12:28	750	-5.525	18.54	73.9	67.5
274	11/17/14 12:28	250	-5.465	18.53	73.9	67.3
276	11/17/14 12:28	750	-5.418	18.53	73.9	67.3
278	11/17/14 12:28	250	-5.358	18.53	73.9	67.3
280	11/17/14 12:28	750	-5.304	18.53	73.9	67.3
282	11/17/14 12:28	250	-5.251	18.53	73.9	67.3
284	11/17/14 12:28	750	-5.204	18.51	74.1	67.3
286	11/17/14 12:28	250	-5.144	18.51	74.1	67.5
288	11/17/14 12:28	750	-5.097	18.51	73.9	67.1
290	11/17/14 12:29	250	-5.044	18.51	74.1	67.1
292	11/17/14 12:29	750	-4.99	18.51	74.1	67.3
294	11/17/14 12:29	250	-4.937	18.51	74.1	67.1
296	11/17/14 12:29	750	-4.883	18.51	74.1	67.3
298	11/17/14 12:29	250	-4.83	18.51	74.1	67.1
300	11/17/14 12:29	750	-4.777	18.51	74.1	67.1
302	11/17/14 12:29	250	-4.723	18.49	74.1	67.1
304	11/17/14 12:29	750	-4.67	18.49	74.1	67.1
306	11/17/14 12:29	250	-4.616	18.49	74.1	67.1
308	11/17/14 12:29	750	-4.563	18.49	74.1	67.1
310	11/17/14 12:29	250	-4.516	18.49	74.3	67.1

312	11/17/14 12:29	750	-4.456	18.49	74.5	67.1
314	11/17/14 12:29	250	-4.402	18.48	74.3	67.1
316	11/17/14 12:29	750	-4.349	18.49	74.5	67.1
318	11/17/14 12:29	250	-4.302	18.49	74.5	67.1
320	11/17/14 12:29	750	-4.249	18.49	74.3	67.1
322	11/17/14 12:29	250	-4.195	18.49	74.5	67.1
324	11/17/14 12:29	750	-4.149	18.51	74.5	67.1
326	11/17/14 12:29	250	-4.095	18.49	74.5	67.1
328	11/17/14 12:29	750	-4.035	18.49	74.5	67.1
330	11/17/14 12:29	250	-3.982	18.48	74.5	67.1
332	11/17/14 12:29	750	-3.928	18.48	74.5	67.1
334	11/17/14 12:29	250	-3.875	18.48	74.5	67.1
336	11/17/14 12:29	750	-3.821	18.46	74.5	67.1
338	11/17/14 12:29	250	-3.768	18.46	74.5	67.1
340	11/17/14 12:29	750	-3.714	18.46	74.7	67.1
342	11/17/14 12:29	250	-3.661	18.46	74.5	67.1
344	11/17/14 12:29	750	-3.607	18.46	74.5	66.9
346	11/17/14 12:29	250	-3.561	18.46	74.5	66.9
348	11/17/14 12:29	750	-3.501	18.46	74.5	67.1
350	11/17/14 12:29	250	-3.447	18.46	74.7	67.1
352	11/17/14 12:29	750	-3.394	18.46	74.7	67.1
354	11/17/14 12:29	250	-3.34	18.46	74.7	67.1
356	11/17/14 12:29	750	-3.293	18.46	74.7	66.9
358	11/17/14 12:29	250	-3.233	18.46	74.8	66.9
360	11/17/14 12:29	750	-3.187	18.46	74.8	66.9
362	11/17/14 12:29	250	-3.133	18.46	74.8	67.1
364	11/17/14 12:29	750	-3.08	18.46	75	67.1
366	11/17/14 12:29	250	-3.026	18.46	75	67.1
368	11/17/14 12:29	750	-2.973	18.46	75.2	67.3
370	11/17/14 12:29	250	-2.919	18.46	75.2	67.3
372	11/17/14 12:29	750	-2.866	18.46	75.2	67.1
374	11/17/14 12:29	250	-2.819	18.45	75.2	67.1
376	11/17/14 12:29	750	-2.759	18.45	75.4	67.5
378	11/17/14 12:29	250	-2.712	18.45	75.4	67.3
380	11/17/14 12:29	750	-2.659	18.45	75.4	67.3
382	11/17/14 12:29	250	-2.605	18.45	75.4	67.5
384	11/17/14 12:29	750	-2.552	18.45	75.4	67.5
386	11/17/14 12:29	250	-2.492	18.45	75.4	67.1
388	11/17/14 12:29	750	-2.445	18.45	75.4	67.1
390	11/17/14 12:29	250	-2.385	18.45	75.4	67.1
392	11/17/14 12:29	750	-2.338	18.43	75.4	67.1
394	11/17/14 12:29	250	-2.285	18.43	75.4	67.1
396	11/17/14 12:29	750	-2.231	18.43	75.4	67.1

398	11/17/14 12:29	250	-2.178	18.43	75.4	67.1
400	11/17/14 12:29	750	-2.124	18.43	75.4	67.1
402	11/17/14 12:29	250	-2.071	18.43	75.4	67.1
404	11/17/14 12:29	750	-2.017	18.43	75.4	67.1
406	11/17/14 12:29	250	-1.971	18.43	75.4	67.1
408	11/17/14 12:29	750	-1.911	18.43	75.4	67.1
410	11/17/14 12:29	250	-1.864	18.43	75.4	67.1
412	11/17/14 12:29	750	-1.81	18.42	75.4	67.1
414	11/17/14 12:29	250	-1.757	18.42	75.4	67.1
416	11/17/14 12:29	750	-1.704	18.42	75.4	67.1
418	11/17/14 12:29	250	-1.65	18.42	75.4	67.1
420	11/17/14 12:29	750	-1.597	18.42	75.4	67.1
422	11/17/14 12:29	250	-1.543	18.42	75.4	67.1
424	11/17/14 12:29	750	-1.49	18.42	75.4	66.9
426	11/17/14 12:29	250	-1.436	18.4	75.4	67.1
428	11/17/14 12:29	750	-1.396	18.42	75.6	67.1
430	11/17/14 12:29	250	-1.336	18.42	75.6	67.1
432	11/17/14 12:29	750	-1.283	18.43	75.6	67.1
434	11/17/14 12:29	250	-1.229	18.42	75.6	67.1
436	11/17/14 12:29	750	-1.176	18.42	75.7	67.1
438	11/17/14 12:29	250	-1.129	18.42	75.6	67.1
440	11/17/14 12:29	750	-1.069	18.43	75.7	67.1
442	11/17/14 12:29	250	-1.022	18.42	75.7	67.1
444	11/17/14 12:29	750	-0.969	18.42	75.7	67.3
446	11/17/14 12:29	250	-0.915	18.42	75.7	67.3
448	11/17/14 12:29	750	-0.862	18.42	75.7	67.3
450	11/17/14 12:29	250	-0.808	18.4	75.7	67.3
452	11/17/14 12:29	750	-0.748	18.4	75.9	67.3
454	11/17/14 12:29	250	-0.695	18.4	75.7	67.3
456	11/17/14 12:29	750	-0.648	18.39	75.9	67.3
458	11/17/14 12:29	250	-0.588	18.4	75.9	67.3
460	11/17/14 12:29	750	-0.541	18.39	75.9	67.1
462	11/17/14 12:29	250	-0.494	18.4	75.9	67.1
464	11/17/14 12:29	750	-0.441	18.4	75.9	67.1
466	11/17/14 12:29	250	-0.387	18.42	75.9	67.1
468	11/17/14 12:29	750	-0.334	18.4	75.9	67.1
470	11/17/14 12:29	250	-0.281	18.4	75.9	67.3
472	11/17/14 12:29	750	-0.227	18.4	75.9	67.1
474	11/17/14 12:29	250	-0.18	18.4	75.9	67.1
476	11/17/14 12:29	750	-0.12	18.4	75.9	67.1
478	11/17/14 12:29	250	-0.073	18.4	75.9	67.1
480	11/17/14 12:29	750	-0.013	18.4	75.9	67.1
482	11/17/14 12:29	250	0.04	18.4	75.9	67.1

484	11/17/14 12:29	750	0.094	18.39	75.9	67.1
486	11/17/14 12:29	250	0.147	18.37	75.9	67.1
488	11/17/14 12:29	750	0.194	18.37	75.9	67.1
490	11/17/14 12:29	250	0.254	18.39	75.9	67.1

1/64-inch Regular Orifice Plate

Vendor	GRAPHTEC Corp.						
Model	GL820						
Version	Ver1.03						
Sampling interval	250ms						
Total data points	2154						
Start time	11/17/2014	11:50:32					
End time	11/17/2014	11:59:30					
Trigger time	11/17/2014	11:50:32					
AMP settings							
CH	Signal name	Input	Range	Filter	Span		
CH1	P TANK	DC	50V	Off	-64.106	69.503	[psi]
CH2	P UPSTREAM	DC	50V	Off	149.5	-161.75	[psi]
CH3	T TANK	TEMP	TC_K	Off	3000	-200	[degF]
CH4	T UPSTREAM	TEMP	TC_K	Off	3000	-200	[degF]
Logic/Pulse	Off						
Data							
Number	Date&Time	ms	CH1	CH2	CH3	CH4	
NO.	Time	ms	psi	psi	degF	degF	
50	11/17/14 11:50	250	-11.651	19.69	64.9	67.3	
60	11/17/14 11:50	750	-11.657	19.54	64.9	67.3	
70	11/17/14 11:50	250	-11.657	19.43	65.1	67.3	
80	11/17/14 11:50	750	-11.651	19.35	65.1	67.1	
90	11/17/14 11:50	250	-11.651	19.27	65.1	67.3	
100	11/17/14 11:50	750	-11.644	19.21	65.3	67.3	
110	11/17/14 11:50	250	-11.657	19.18	65.3	67.3	
120	11/17/14 11:51	750	-11.644	19.12	65.3	67.1	
130	11/17/14 11:51	250	-11.637	19.07	65.3	67.1	
140	11/17/14 11:51	750	-11.637	19.04	65.3	67.1	
150	11/17/14 11:51	250	-11.631	19.01	65.7	67.1	
160	11/17/14 11:51	750	-11.611	18.98	65.5	67.1	
170	11/17/14 11:51	250	-11.597	18.96	65.7	67.1	
180	11/17/14 11:51	750	-11.571	18.92	65.7	67.1	
190	11/17/14 11:51	250	-11.544	18.9	65.7	66.9	
200	11/17/14 11:51	750	-11.504	18.88	65.7	67.1	
210	11/17/14 11:51	250	-11.45	18.85	65.7	66.9	
220	11/17/14 11:51	750	-11.404	18.85	65.7	67.1	
230	11/17/14 11:51	250	-11.35	18.84	65.7	67.1	
240	11/17/14 11:51	750	-11.29	18.82	65.7	66.9	
250	11/17/14 11:51	250	-11.23	18.81	65.8	67.1	
260	11/17/14 11:51	750	-11.163	18.79	65.8	66.9	

270	11/17/14 11:51	250	-11.103	18.76	65.8	66.9
280	11/17/14 11:51	750	-11.049	18.76	65.8	66.9
290	11/17/14 11:51	250	-10.989	18.74	66	66.9
300	11/17/14 11:51	750	-10.923	18.71	66	66.9
310	11/17/14 11:51	250	-10.869	18.71	66	66.9
320	11/17/14 11:51	750	-10.809	18.71	66.2	66.9
330	11/17/14 11:51	250	-10.756	18.7	66.2	67.1
340	11/17/14 11:51	750	-10.689	18.7	66.2	67.1
350	11/17/14 11:51	250	-10.629	18.68	66.2	66.9
360	11/17/14 11:52	750	-10.568	18.67	66.4	67.1
370	11/17/14 11:52	250	-10.508	18.65	66.4	67.1
380	11/17/14 11:52	750	-10.448	18.63	66.2	66.9
390	11/17/14 11:52	250	-10.388	18.63	66.4	67.1
400	11/17/14 11:52	750	-10.328	18.63	66.4	67.1
410	11/17/14 11:52	250	-10.268	18.62	66.4	66.9
420	11/17/14 11:52	750	-10.208	18.6	66.6	66.9
430	11/17/14 11:52	250	-10.148	18.57	66.6	66.9
440	11/17/14 11:52	750	-10.094	18.59	66.6	67.1
450	11/17/14 11:52	250	-10.027	18.57	66.6	66.9
460	11/17/14 11:52	750	-9.967	18.57	66.6	67.1
470	11/17/14 11:52	250	-9.907	18.56	66.7	67.1
480	11/17/14 11:52	750	-9.847	18.57	66.6	67.1
490	11/17/14 11:52	250	-9.787	18.54	66.6	67.1
500	11/17/14 11:52	750	-9.727	18.54	66.7	67.1
510	11/17/14 11:52	250	-9.667	18.53	66.6	66.9
520	11/17/14 11:52	750	-9.606	18.53	66.7	66.9
530	11/17/14 11:52	250	-9.546	18.51	66.7	66.9
540	11/17/14 11:52	750	-9.486	18.51	66.6	66.9
550	11/17/14 11:52	250	-9.426	18.51	66.6	66.9
560	11/17/14 11:52	750	-9.366	18.49	66.9	67.1
570	11/17/14 11:52	250	-9.306	18.49	66.9	67.1
580	11/17/14 11:52	750	-9.239	18.46	66.9	67.1
590	11/17/14 11:52	250	-9.186	18.48	66.9	66.9
600	11/17/14 11:53	750	-9.119	18.46	66.7	66.9
610	11/17/14 11:53	250	-9.065	18.46	66.9	66.9
620	11/17/14 11:53	750	-9.005	18.46	66.7	66.9
630	11/17/14 11:53	250	-8.952	18.46	66.7	66.9
640	11/17/14 11:53	750	-8.885	18.46	66.9	66.9
650	11/17/14 11:53	250	-8.832	18.45	66.9	66.9
660	11/17/14 11:53	750	-8.771	18.43	67.1	67.1
670	11/17/14 11:53	250	-8.711	18.43	66.9	66.9
680	11/17/14 11:53	750	-8.651	18.43	66.9	66.9
690	11/17/14 11:53	250	-8.591	18.42	66.9	66.9

700	11/17/14 11:53	750	-8.524	18.42	66.9	66.9
710	11/17/14 11:53	250	-8.471	18.42	67.1	66.9
720	11/17/14 11:53	750	-8.411	18.42	67.1	66.9
730	11/17/14 11:53	250	-8.351	18.4	66.9	66.9
740	11/17/14 11:53	750	-8.297	18.4	67.1	66.9
750	11/17/14 11:53	250	-8.23	18.39	67.1	66.9
760	11/17/14 11:53	750	-8.17	18.37	67.3	66.9
770	11/17/14 11:53	250	-8.11	18.37	67.3	66.9
780	11/17/14 11:53	750	-8.057	18.39	67.3	66.9
790	11/17/14 11:53	250	-7.997	18.37	67.3	66.9
800	11/17/14 11:53	750	-7.93	18.37	67.5	66.9
810	11/17/14 11:53	250	-7.876	18.37	67.3	66.9
820	11/17/14 11:53	750	-7.816	18.37	67.5	66.9
830	11/17/14 11:53	250	-7.749	18.34	67.5	66.9
840	11/17/14 11:54	750	-7.709	18.37	67.3	66.9
850	11/17/14 11:54	250	-7.636	18.35	67.5	66.9
860	11/17/14 11:54	750	-7.582	18.35	67.5	66.9
870	11/17/14 11:54	250	-7.522	18.35	67.6	67.1
880	11/17/14 11:54	750	-7.462	18.34	67.6	67.1
890	11/17/14 11:54	250	-7.395	18.32	67.6	67.1
900	11/17/14 11:54	750	-7.342	18.32	67.6	67.1
910	11/17/14 11:54	250	-7.282	18.34	67.6	66.9
920	11/17/14 11:54	750	-7.215	18.31	67.6	67.1
930	11/17/14 11:54	250	-7.161	18.32	67.6	67.1
940	11/17/14 11:54	750	-7.101	18.29	67.6	66.9
950	11/17/14 11:54	250	-7.048	18.31	67.6	66.9
960	11/17/14 11:54	750	-6.988	18.31	67.6	66.9
970	11/17/14 11:54	250	-6.928	18.31	67.6	67.1
980	11/17/14 11:54	750	-6.868	18.31	67.6	66.9
990	11/17/14 11:54	250	-6.807	18.29	67.6	66.9
1000	11/17/14 11:54	750	-6.747	18.29	67.6	66.9
1010	11/17/14 11:54	250	-6.687	18.29	67.6	66.9
1020	11/17/14 11:54	750	-6.627	18.29	67.8	67.1
1030	11/17/14 11:54	250	-6.567	18.29	67.6	66.9
1040	11/17/14 11:54	750	-6.513	18.29	67.8	67.1
1050	11/17/14 11:54	250	-6.46	18.29	67.6	66.9
1060	11/17/14 11:54	750	-6.393	18.29	67.6	66.9
1070	11/17/14 11:54	250	-6.333	18.28	67.6	66.9
1080	11/17/14 11:55	750	-6.273	18.28	68	67.1
1090	11/17/14 11:55	250	-6.213	18.28	68	67.1
1100	11/17/14 11:55	750	-6.153	18.28	68	67.1
1110	11/17/14 11:55	250	-6.093	18.26	68	67.1
1120	11/17/14 11:55	750	-6.026	18.25	68	66.9

1130	11/17/14 11:55	250	-5.979	18.26	68	66.9
1140	11/17/14 11:55	750	-5.919	18.25	68	66.9
1150	11/17/14 11:55	250	-5.865	18.26	68	66.9
1160	11/17/14 11:55	750	-5.799	18.25	68	66.9
1170	11/17/14 11:55	250	-5.745	18.25	67.8	66.9
1180	11/17/14 11:55	750	-5.685	18.23	68	66.9
1190	11/17/14 11:55	250	-5.618	18.25	68	66.9
1200	11/17/14 11:55	750	-5.565	18.23	68	66.9
1210	11/17/14 11:55	250	-5.505	18.23	68	66.9
1220	11/17/14 11:55	750	-5.445	18.23	68.2	67.1
1230	11/17/14 11:55	250	-5.384	18.21	68	66.9
1240	11/17/14 11:55	750	-5.324	18.21	68	66.9
1250	11/17/14 11:55	250	-5.264	18.21	68.2	66.9
1260	11/17/14 11:55	750	-5.211	18.21	68.2	66.9
1270	11/17/14 11:55	250	-5.144	18.21	68	66.9
1280	11/17/14 11:55	750	-5.091	18.21	68.2	66.9
1290	11/17/14 11:55	250	-5.03	18.2	68.2	66.9
1300	11/17/14 11:55	750	-4.97	18.2	68.2	66.9
1310	11/17/14 11:55	250	-4.91	18.2	68.4	67.1
1320	11/17/14 11:56	750	-4.85	18.2	68.4	67.1
1330	11/17/14 11:56	250	-4.79	18.2	68.4	66.9
1340	11/17/14 11:56	750	-4.736	18.2	68.4	66.9
1350	11/17/14 11:56	250	-4.676	18.2	68.4	66.9
1360	11/17/14 11:56	750	-4.616	18.18	68.4	66.9
1370	11/17/14 11:56	250	-4.549	18.2	68.4	66.9
1380	11/17/14 11:56	750	-4.496	18.18	68.5	66.9
1390	11/17/14 11:56	250	-4.443	18.18	68.4	66.9
1400	11/17/14 11:56	750	-4.369	18.17	68.5	66.9
1410	11/17/14 11:56	250	-4.322	18.18	68.5	66.9
1420	11/17/14 11:56	750	-4.255	18.18	68.4	66.9
1430	11/17/14 11:56	250	-4.202	18.18	68.5	66.9
1440	11/17/14 11:56	750	-4.149	18.18	68.7	66.9
1450	11/17/14 11:56	250	-4.082	18.17	68.5	66.9
1460	11/17/14 11:56	750	-4.022	18.17	68.7	66.9
1470	11/17/14 11:56	250	-3.962	18.17	68.7	66.9
1480	11/17/14 11:56	750	-3.901	18.17	68.5	66.9
1490	11/17/14 11:56	250	-3.848	18.17	68.5	66.9
1500	11/17/14 11:56	750	-3.781	18.17	68.7	66.9
1510	11/17/14 11:56	250	-3.728	18.17	68.7	66.9
1520	11/17/14 11:56	750	-3.668	18.17	68.5	66.9
1530	11/17/14 11:56	250	-3.607	18.15	68.7	66.9
1540	11/17/14 11:56	750	-3.554	18.15	68.7	66.9
1550	11/17/14 11:56	250	-3.487	18.15	68.9	67.1

1560	11/17/14 11:57	750	-3.427	18.15	68.9	67.1
1570	11/17/14 11:57	250	-3.374	18.17	68.9	66.9
1580	11/17/14 11:57	750	-3.307	18.12	68.9	67.1
1590	11/17/14 11:57	250	-3.253	18.14	68.9	67.1
1600	11/17/14 11:57	750	-3.193	18.15	68.9	67.1
1610	11/17/14 11:57	250	-3.133	18.14	68.9	66.9
1620	11/17/14 11:57	750	-3.08	18.14	68.9	66.9
1630	11/17/14 11:57	250	-3.013	18.14	68.9	66.9
1640	11/17/14 11:57	750	-2.953	18.12	68.9	66.9
1650	11/17/14 11:57	250	-2.899	18.14	69.1	67.1
1660	11/17/14 11:57	750	-2.846	18.14	68.9	66.9
1670	11/17/14 11:57	250	-2.786	18.14	69.1	67.1
1680	11/17/14 11:57	750	-2.719	18.12	69.1	66.9
1690	11/17/14 11:57	250	-2.666	18.12	69.1	66.9
1700	11/17/14 11:57	750	-2.605	18.14	69.1	66.9
1710	11/17/14 11:57	250	-2.545	18.12	69.1	66.9
1720	11/17/14 11:57	750	-2.492	18.12	69.3	66.9
1730	11/17/14 11:57	250	-2.425	18.12	69.3	66.9
1740	11/17/14 11:57	750	-2.372	18.12	69.1	66.9
1750	11/17/14 11:57	250	-2.311	18.12	69.3	66.9
1760	11/17/14 11:57	750	-2.251	18.12	69.3	66.9
1770	11/17/14 11:57	250	-2.198	18.12	69.3	66.9
1780	11/17/14 11:57	750	-2.131	18.11	69.3	67.1
1790	11/17/14 11:57	250	-2.084	18.12	69.3	67.1
1800	11/17/14 11:58	750	-2.017	18.12	69.3	67.1
1810	11/17/14 11:58	250	-1.964	18.11	69.3	66.9
1820	11/17/14 11:58	750	-1.904	18.11	69.3	67.1
1830	11/17/14 11:58	250	-1.837	18.11	69.3	67.1
1840	11/17/14 11:58	750	-1.784	18.11	69.3	67.1
1850	11/17/14 11:58	250	-1.724	18.11	69.3	66.9
1860	11/17/14 11:58	750	-1.663	18.11	69.3	67.1
1870	11/17/14 11:58	250	-1.603	18.11	69.3	66.9
1880	11/17/14 11:58	750	-1.543	18.11	69.3	66.9
1890	11/17/14 11:58	250	-1.49	18.11	69.4	67.1
1900	11/17/14 11:58	750	-1.43	18.11	69.4	67.1
1910	11/17/14 11:58	250	-1.369	18.09	69.4	67.1
1920	11/17/14 11:58	750	-1.309	18.09	69.4	67.1
1930	11/17/14 11:58	250	-1.249	18.09	69.4	66.9
1940	11/17/14 11:58	750	-1.196	18.09	69.4	66.9
1950	11/17/14 11:58	250	-1.136	18.09	69.4	66.9
1960	11/17/14 11:58	750	-1.069	18.07	69.4	66.9
1970	11/17/14 11:58	250	-1.015	18.09	69.4	67.1
1980	11/17/14 11:58	750	-0.955	18.07	69.4	66.9

1990	11/17/14 11:58	250	-0.895	18.07	69.4	66.9
2000	11/17/14 11:58	750	-0.842	18.07	69.6	66.9
2010	11/17/14 11:58	250	-0.788	18.09	69.4	66.9
2020	11/17/14 11:58	750	-0.728	18.09	69.6	66.9
2030	11/17/14 11:58	250	-0.661	18.09	69.6	67.1
2040	11/17/14 11:59	750	-0.601	18.07	69.6	67.1
2050	11/17/14 11:59	250	-0.548	18.07	69.6	66.9
2060	11/17/14 11:59	750	-0.481	18.07	69.6	67.1
2070	11/17/14 11:59	250	-0.434	18.07	69.8	66.9
2080	11/17/14 11:59	750	-0.367	18.06	69.8	66.9
2090	11/17/14 11:59	250	-0.314	18.07	69.8	66.9
2100	11/17/14 11:59	750	-0.247	18.06	69.8	66.9
2110	11/17/14 11:59	250	-0.187	18.06	69.6	66.9
2120	11/17/14 11:59	750	-0.127	18.06	69.8	66.9
2130	11/17/14 11:59	250	-0.073	18.06	69.8	66.9
2140	11/17/14 11:59	750	-0.007	18.06	69.8	66.9
2150	11/17/14 11:59	250	0.04	18.07	69.8	66.9

1/64-inch Chamfered Orifice Plate

Vendor	GRAPHTEC Corp.						
Model	GL820						
Version	Ver1.03						
Sampling interval	250ms						
Total data points	1710						
Start time	11/17/2014	13:13:16					
End time	11/17/2014	13:20:24					
Trigger time	11/17/2014	13:13:17					
AMP settings							
CH	Signal name	Input	Range	Filter	Span		
CH1	P TANK	DC	50V	Off	-64.106	69.503	[psi]
CH2	P UPSTREAM	DC	50V	Off	149.5	-161.75	[psi]
CH3	T TANK	TEMP	TC_K	Off	3000	-200	[degF]
CH4	T UPSTREAM	TEMP	TC_K	Off	3000	-200	[degF]
Logic/Pulse	Off						
Data							
Number	Date&Time	ms	CH1	CH2	CH3	CH4	
NO.	Time	ms	psi	psi	degF	degF	
50	11/17/14 11:50	250	-11.651	19.69	64.9	67.3	
60	11/17/14 11:50	750	-11.657	19.54	64.9	67.3	
70	11/17/14 11:50	250	-11.657	19.43	65.1	67.3	
80	11/17/14 11:50	750	-11.651	19.35	65.1	67.1	
90	11/17/14 11:50	250	-11.651	19.27	65.1	67.3	
100	11/17/14 11:50	750	-11.644	19.21	65.3	67.3	
110	11/17/14 11:50	250	-11.657	19.18	65.3	67.3	
120	11/17/14 11:51	750	-11.644	19.12	65.3	67.1	
130	11/17/14 11:51	250	-11.637	19.07	65.3	67.1	
140	11/17/14 11:51	750	-11.637	19.04	65.3	67.1	
150	11/17/14 11:51	250	-11.631	19.01	65.7	67.1	
160	11/17/14 11:51	750	-11.611	18.98	65.5	67.1	
170	11/17/14 11:51	250	-11.597	18.96	65.7	67.1	
180	11/17/14 11:51	750	-11.571	18.92	65.7	67.1	
190	11/17/14 11:51	250	-11.544	18.9	65.7	66.9	
200	11/17/14 11:51	750	-11.504	18.88	65.7	67.1	
210	11/17/14 11:51	250	-11.45	18.85	65.7	66.9	
220	11/17/14 11:51	750	-11.404	18.85	65.7	67.1	
230	11/17/14 11:51	250	-11.35	18.84	65.7	67.1	
240	11/17/14 11:51	750	-11.29	18.82	65.7	66.9	
250	11/17/14 11:51	250	-11.23	18.81	65.8	67.1	
260	11/17/14 11:51	750	-11.163	18.79	65.8	66.9	
270	11/17/14 11:51	250	-11.103	18.76	65.8	66.9	

280	11/17/14 11:51	750	-11.049	18.76	65.8	66.9
290	11/17/14 11:51	250	-10.989	18.74	66	66.9
300	11/17/14 11:51	750	-10.923	18.71	66	66.9
310	11/17/14 11:51	250	-10.869	18.71	66	66.9
320	11/17/14 11:51	750	-10.809	18.71	66.2	66.9
330	11/17/14 11:51	250	-10.756	18.7	66.2	67.1
340	11/17/14 11:51	750	-10.689	18.7	66.2	67.1
350	11/17/14 11:51	250	-10.629	18.68	66.2	66.9
360	11/17/14 11:52	750	-10.568	18.67	66.4	67.1
370	11/17/14 11:52	250	-10.508	18.65	66.4	67.1
380	11/17/14 11:52	750	-10.448	18.63	66.2	66.9
390	11/17/14 11:52	250	-10.388	18.63	66.4	67.1
400	11/17/14 11:52	750	-10.328	18.63	66.4	67.1
410	11/17/14 11:52	250	-10.268	18.62	66.4	66.9
420	11/17/14 11:52	750	-10.208	18.6	66.6	66.9
430	11/17/14 11:52	250	-10.148	18.57	66.6	66.9
440	11/17/14 11:52	750	-10.094	18.59	66.6	67.1
450	11/17/14 11:52	250	-10.027	18.57	66.6	66.9
460	11/17/14 11:52	750	-9.967	18.57	66.6	67.1
470	11/17/14 11:52	250	-9.907	18.56	66.7	67.1
480	11/17/14 11:52	750	-9.847	18.57	66.6	67.1
490	11/17/14 11:52	250	-9.787	18.54	66.6	67.1
500	11/17/14 11:52	750	-9.727	18.54	66.7	67.1
510	11/17/14 11:52	250	-9.667	18.53	66.6	66.9
520	11/17/14 11:52	750	-9.606	18.53	66.7	66.9
530	11/17/14 11:52	250	-9.546	18.51	66.7	66.9
540	11/17/14 11:52	750	-9.486	18.51	66.6	66.9
550	11/17/14 11:52	250	-9.426	18.51	66.6	66.9
560	11/17/14 11:52	750	-9.366	18.49	66.9	67.1
570	11/17/14 11:52	250	-9.306	18.49	66.9	67.1
580	11/17/14 11:52	750	-9.239	18.46	66.9	67.1
590	11/17/14 11:52	250	-9.186	18.48	66.9	66.9
600	11/17/14 11:53	750	-9.119	18.46	66.7	66.9
610	11/17/14 11:53	250	-9.065	18.46	66.9	66.9
620	11/17/14 11:53	750	-9.005	18.46	66.7	66.9
630	11/17/14 11:53	250	-8.952	18.46	66.7	66.9
640	11/17/14 11:53	750	-8.885	18.46	66.9	66.9
650	11/17/14 11:53	250	-8.832	18.45	66.9	66.9
660	11/17/14 11:53	750	-8.771	18.43	67.1	67.1
670	11/17/14 11:53	250	-8.711	18.43	66.9	66.9
680	11/17/14 11:53	750	-8.651	18.43	66.9	66.9
690	11/17/14 11:53	250	-8.591	18.42	66.9	66.9
700	11/17/14 11:53	750	-8.524	18.42	66.9	66.9

710	11/17/14 11:53	250	-8.471	18.42	67.1	66.9
720	11/17/14 11:53	750	-8.411	18.42	67.1	66.9
730	11/17/14 11:53	250	-8.351	18.4	66.9	66.9
740	11/17/14 11:53	750	-8.297	18.4	67.1	66.9
750	11/17/14 11:53	250	-8.23	18.39	67.1	66.9
760	11/17/14 11:53	750	-8.17	18.37	67.3	66.9
770	11/17/14 11:53	250	-8.11	18.37	67.3	66.9
780	11/17/14 11:53	750	-8.057	18.39	67.3	66.9
790	11/17/14 11:53	250	-7.997	18.37	67.3	66.9
800	11/17/14 11:53	750	-7.93	18.37	67.5	66.9
810	11/17/14 11:53	250	-7.876	18.37	67.3	66.9
820	11/17/14 11:53	750	-7.816	18.37	67.5	66.9
830	11/17/14 11:53	250	-7.749	18.34	67.5	66.9
840	11/17/14 11:54	750	-7.709	18.37	67.3	66.9
850	11/17/14 11:54	250	-7.636	18.35	67.5	66.9
860	11/17/14 11:54	750	-7.582	18.35	67.5	66.9
870	11/17/14 11:54	250	-7.522	18.35	67.6	67.1
880	11/17/14 11:54	750	-7.462	18.34	67.6	67.1
890	11/17/14 11:54	250	-7.395	18.32	67.6	67.1
900	11/17/14 11:54	750	-7.342	18.32	67.6	67.1
910	11/17/14 11:54	250	-7.282	18.34	67.6	66.9
920	11/17/14 11:54	750	-7.215	18.31	67.6	67.1
930	11/17/14 11:54	250	-7.161	18.32	67.6	67.1
940	11/17/14 11:54	750	-7.101	18.29	67.6	66.9
950	11/17/14 11:54	250	-7.048	18.31	67.6	66.9
960	11/17/14 11:54	750	-6.988	18.31	67.6	66.9
970	11/17/14 11:54	250	-6.928	18.31	67.6	67.1
980	11/17/14 11:54	750	-6.868	18.31	67.6	66.9
990	11/17/14 11:54	250	-6.807	18.29	67.6	66.9
1000	11/17/14 11:54	750	-6.747	18.29	67.6	66.9
1010	11/17/14 11:54	250	-6.687	18.29	67.6	66.9
1020	11/17/14 11:54	750	-6.627	18.29	67.8	67.1
1030	11/17/14 11:54	250	-6.567	18.29	67.6	66.9
1040	11/17/14 11:54	750	-6.513	18.29	67.8	67.1
1050	11/17/14 11:54	250	-6.46	18.29	67.6	66.9
1060	11/17/14 11:54	750	-6.393	18.29	67.6	66.9
1070	11/17/14 11:54	250	-6.333	18.28	67.6	66.9
1080	11/17/14 11:55	750	-6.273	18.28	68	67.1
1090	11/17/14 11:55	250	-6.213	18.28	68	67.1
1100	11/17/14 11:55	750	-6.153	18.28	68	67.1
1110	11/17/14 11:55	250	-6.093	18.26	68	67.1
1120	11/17/14 11:55	750	-6.026	18.25	68	66.9
1130	11/17/14 11:55	250	-5.979	18.26	68	66.9

1140	11/17/14 11:55	750	-5.919	18.25	68	66.9
1150	11/17/14 11:55	250	-5.865	18.26	68	66.9
1160	11/17/14 11:55	750	-5.799	18.25	68	66.9
1170	11/17/14 11:55	250	-5.745	18.25	67.8	66.9
1180	11/17/14 11:55	750	-5.685	18.23	68	66.9
1190	11/17/14 11:55	250	-5.618	18.25	68	66.9
1200	11/17/14 11:55	750	-5.565	18.23	68	66.9
1210	11/17/14 11:55	250	-5.505	18.23	68	66.9
1220	11/17/14 11:55	750	-5.445	18.23	68.2	67.1
1230	11/17/14 11:55	250	-5.384	18.21	68	66.9
1240	11/17/14 11:55	750	-5.324	18.21	68	66.9
1250	11/17/14 11:55	250	-5.264	18.21	68.2	66.9
1260	11/17/14 11:55	750	-5.211	18.21	68.2	66.9
1270	11/17/14 11:55	250	-5.144	18.21	68	66.9
1280	11/17/14 11:55	750	-5.091	18.21	68.2	66.9
1290	11/17/14 11:55	250	-5.03	18.2	68.2	66.9
1300	11/17/14 11:55	750	-4.97	18.2	68.2	66.9
1310	11/17/14 11:55	250	-4.91	18.2	68.4	67.1
1320	11/17/14 11:56	750	-4.85	18.2	68.4	67.1
1330	11/17/14 11:56	250	-4.79	18.2	68.4	66.9
1340	11/17/14 11:56	750	-4.736	18.2	68.4	66.9
1350	11/17/14 11:56	250	-4.676	18.2	68.4	66.9
1360	11/17/14 11:56	750	-4.616	18.18	68.4	66.9
1370	11/17/14 11:56	250	-4.549	18.2	68.4	66.9
1380	11/17/14 11:56	750	-4.496	18.18	68.5	66.9
1390	11/17/14 11:56	250	-4.443	18.18	68.4	66.9
1400	11/17/14 11:56	750	-4.369	18.17	68.5	66.9
1410	11/17/14 11:56	250	-4.322	18.18	68.5	66.9
1420	11/17/14 11:56	750	-4.255	18.18	68.4	66.9
1430	11/17/14 11:56	250	-4.202	18.18	68.5	66.9
1440	11/17/14 11:56	750	-4.149	18.18	68.7	66.9
1450	11/17/14 11:56	250	-4.082	18.17	68.5	66.9
1460	11/17/14 11:56	750	-4.022	18.17	68.7	66.9
1470	11/17/14 11:56	250	-3.962	18.17	68.7	66.9
1480	11/17/14 11:56	750	-3.901	18.17	68.5	66.9
1490	11/17/14 11:56	250	-3.848	18.17	68.5	66.9
1500	11/17/14 11:56	750	-3.781	18.17	68.7	66.9
1510	11/17/14 11:56	250	-3.728	18.17	68.7	66.9
1520	11/17/14 11:56	750	-3.668	18.17	68.5	66.9
1530	11/17/14 11:56	250	-3.607	18.15	68.7	66.9
1540	11/17/14 11:56	750	-3.554	18.15	68.7	66.9
1550	11/17/14 11:56	250	-3.487	18.15	68.9	67.1
1560	11/17/14 11:57	750	-3.427	18.15	68.9	67.1

1570	11/17/14 11:57	250	-3.374	18.17	68.9	66.9
1580	11/17/14 11:57	750	-3.307	18.12	68.9	67.1
1590	11/17/14 11:57	250	-3.253	18.14	68.9	67.1
1600	11/17/14 11:57	750	-3.193	18.15	68.9	67.1
1610	11/17/14 11:57	250	-3.133	18.14	68.9	66.9
1620	11/17/14 11:57	750	-3.08	18.14	68.9	66.9
1630	11/17/14 11:57	250	-3.013	18.14	68.9	66.9
1640	11/17/14 11:57	750	-2.953	18.12	68.9	66.9
1650	11/17/14 11:57	250	-2.899	18.14	69.1	67.1
1660	11/17/14 11:57	750	-2.846	18.14	68.9	66.9
1670	11/17/14 11:57	250	-2.786	18.14	69.1	67.1
1680	11/17/14 11:57	750	-2.719	18.12	69.1	66.9
1690	11/17/14 11:57	250	-2.666	18.12	69.1	66.9
1700	11/17/14 11:57	750	-2.605	18.14	69.1	66.9
1710	11/17/14 11:57	250	-2.545	18.12	69.1	66.9
1720	11/17/14 11:57	750	-2.492	18.12	69.3	66.9
1730	11/17/14 11:57	250	-2.425	18.12	69.3	66.9
1740	11/17/14 11:57	750	-2.372	18.12	69.1	66.9
1750	11/17/14 11:57	250	-2.311	18.12	69.3	66.9
1760	11/17/14 11:57	750	-2.251	18.12	69.3	66.9
1770	11/17/14 11:57	250	-2.198	18.12	69.3	66.9
1780	11/17/14 11:57	750	-2.131	18.11	69.3	67.1
1790	11/17/14 11:57	250	-2.084	18.12	69.3	67.1
1800	11/17/14 11:58	750	-2.017	18.12	69.3	67.1
1810	11/17/14 11:58	250	-1.964	18.11	69.3	66.9
1820	11/17/14 11:58	750	-1.904	18.11	69.3	67.1
1830	11/17/14 11:58	250	-1.837	18.11	69.3	67.1
1840	11/17/14 11:58	750	-1.784	18.11	69.3	67.1
1850	11/17/14 11:58	250	-1.724	18.11	69.3	66.9
1860	11/17/14 11:58	750	-1.663	18.11	69.3	67.1
1870	11/17/14 11:58	250	-1.603	18.11	69.3	66.9
1880	11/17/14 11:58	750	-1.543	18.11	69.3	66.9
1890	11/17/14 11:58	250	-1.49	18.11	69.4	67.1
1900	11/17/14 11:58	750	-1.43	18.11	69.4	67.1
1910	11/17/14 11:58	250	-1.369	18.09	69.4	67.1
1920	11/17/14 11:58	750	-1.309	18.09	69.4	67.1
1930	11/17/14 11:58	250	-1.249	18.09	69.4	66.9
1940	11/17/14 11:58	750	-1.196	18.09	69.4	66.9
1950	11/17/14 11:58	250	-1.136	18.09	69.4	66.9
1960	11/17/14 11:58	750	-1.069	18.07	69.4	66.9
1970	11/17/14 11:58	250	-1.015	18.09	69.4	67.1
1980	11/17/14 11:58	750	-0.955	18.07	69.4	66.9
1990	11/17/14 11:58	250	-0.895	18.07	69.4	66.9

2000	11/17/14 11:58	750	-0.842	18.07	69.6	66.9
2010	11/17/14 11:58	250	-0.788	18.09	69.4	66.9
2020	11/17/14 11:58	750	-0.728	18.09	69.6	66.9
2030	11/17/14 11:58	250	-0.661	18.09	69.6	67.1
2040	11/17/14 11:59	750	-0.601	18.07	69.6	67.1
2050	11/17/14 11:59	250	-0.548	18.07	69.6	66.9
2060	11/17/14 11:59	750	-0.481	18.07	69.6	67.1
2070	11/17/14 11:59	250	-0.434	18.07	69.8	66.9
2080	11/17/14 11:59	750	-0.367	18.06	69.8	66.9
2090	11/17/14 11:59	250	-0.314	18.07	69.8	66.9
2100	11/17/14 11:59	750	-0.247	18.06	69.8	66.9
2110	11/17/14 11:59	250	-0.187	18.06	69.6	66.9
2120	11/17/14 11:59	750	-0.127	18.06	69.8	66.9
2130	11/17/14 11:59	250	-0.073	18.06	69.8	66.9
2140	11/17/14 11:59	750	-0.007	18.06	69.8	66.9
2150	11/17/14 11:59	250	0.04	18.07	69.8	66.9

Appendix E: Diagrams, Graphs, Tables, etc.

Omega differential pressure transducer wiring diagrams

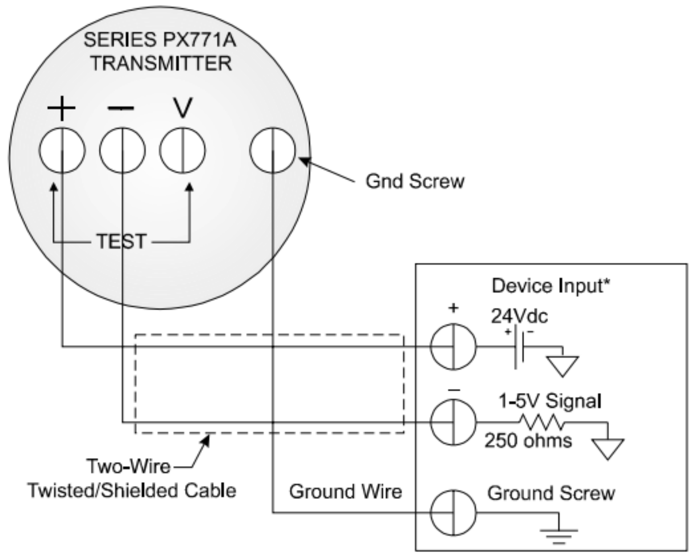

* The device may be an indicator, recorder, tone modulator, etc.
*1 Connect the shield to earth ground or to a shield terminal on the device, if so equipped.
*2 Refer to Figure 3-2 and set the Jumper Block for Current Operation.

Figure 2-2 - Transmitter Wired to Instrument Supply Source (4-20mA Circuit)

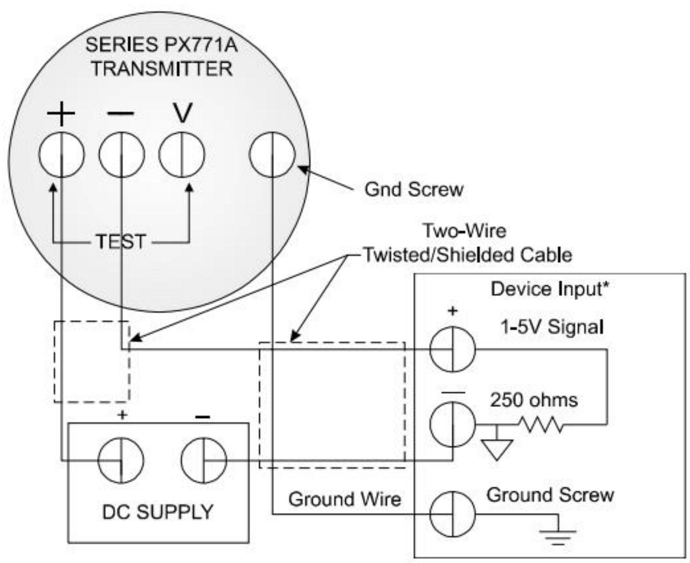

* The device may be an indicator, recorder, tone modulator, etc.
*1 Connect the shield to earth ground or to a shield terminal on the device, if so equipped.
*2 Refer to Figure 3-2 and set the Jumper Block for Current Operation.

Figure 2-3 - Transmitter Wired to External DC Supply (4-20mA Circuit)

Spink's YtSp Graph for d/D

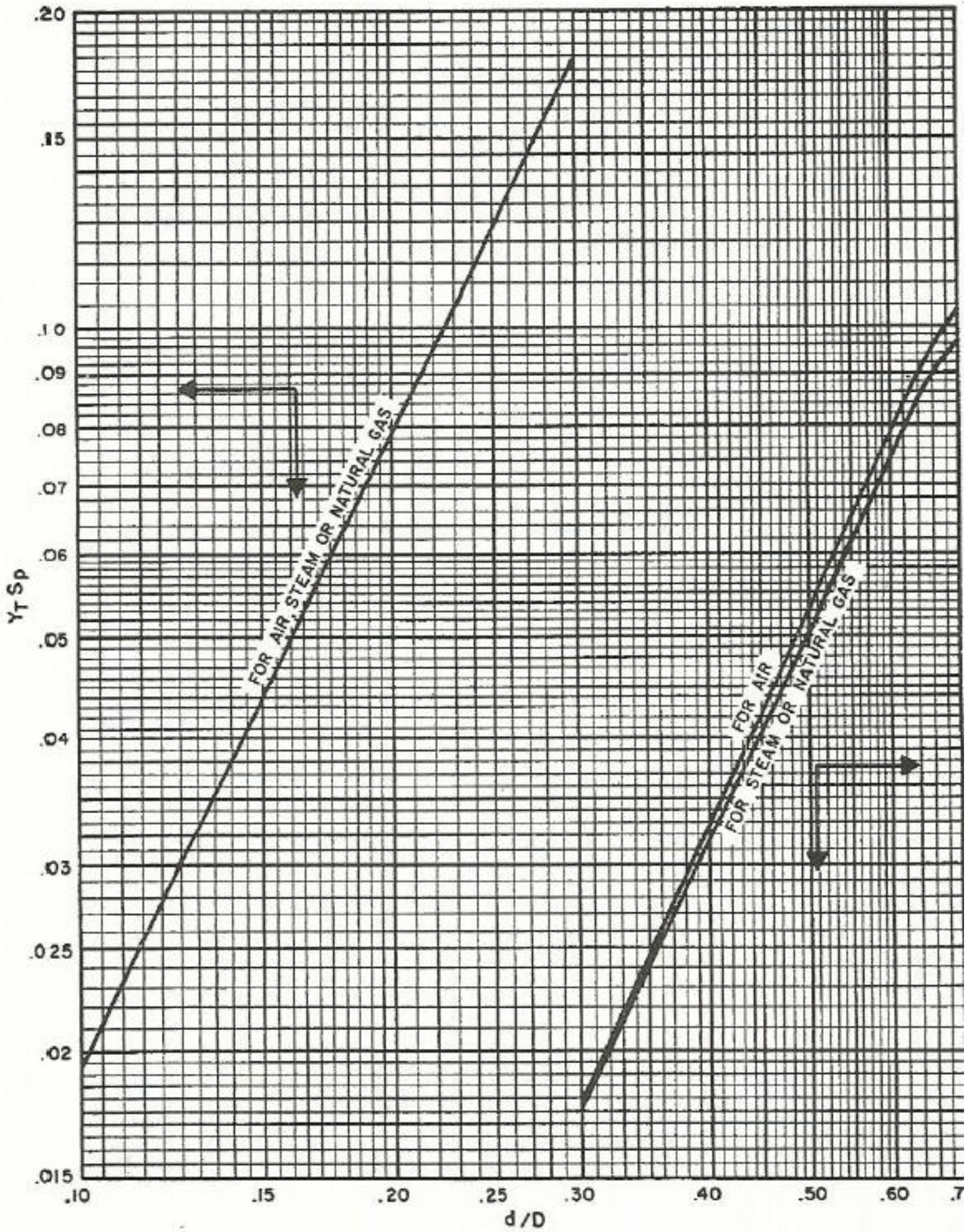

Fig. B-2525 $Y_T S_P$ for Throttling Orifices at Critical Pressure Drop

Pocatello Airport Conditions at Time of Testing

Weather History for KPIH

Nearest airport to Pocatello Regional, ID. See history from more local stations

Monthly Calendar Detailed History

Change the Weather History Date:

November 17 2014 View

Monday, November 17, 2014

Hourly Weather History & Observations

Time (MST)	Temp.	Windchill	Dew Point	Humidity	Pressure	Visibility	Wind Dir	Wind Speed
12:53 PM	19.9 °F	11.1 °F	9.0 °F	62%	30.67 in	10.0 mi	North	6.9 mph

Experimental Apparatus Line Dimensions

	Pipe/Tube/Hose	Material	Line Length	Inside Diameter
Vacuum Pump Line	From vacuum pump to 90 degree bend	Galvanized Steel	27"	1.05"
	From 90 degree bend to ball valve	Galvanized Steel	6.5"	1.05"
	From ball valve to receiver tank	Galvanized Steel	11.75"	1.05"
Upstream of Orifice Plate	From regulator to end of hose	Rubber Hose	118.5"	0.375"
	From end of hose to upstream thermocouple	316 Stainless Steel	3"	0.43"
	From upstream thermocouple to orifice plate	316 Stainless Steel	48.5"	0.43"
	From upstream DPT line to orifice plate	316 Stainless Steel	3.5"	0.43"
	From DPT to swagelok tee	Copper	36"	0.065"
Downstream of Orifice Plate	From orifice plate to receiver tank	316 Stainless Steel	2"	0.62"
	From DPT to receiver tank	Copper	36"	0.065"